Bw Cy

WRDC-TR-90-4017

ADA 221895

Ternary Phase Diagrams of PBZT/Zytel 330/MSA and PBZT/Lubrizol/MSA Solutions

Charles Y-C. Lee
Polymer Branch
WRDC/MLBP
Wright-Patterson AFB, OH 45433-6533

Wansoo Huh
AdTech Systems Research
1342 N. Fairfield Rd
Dayton, OH 45432

S. J. Bai
Research Institute
University of Dayton
300 College Park
Dayton, OH 45469

January 1990

Interim Report for Period January 1989 to December 1989

Best Available Copy

20040219 296

NOTICE

WHEN GOVERNMENT DRAWINGS, SPECIFICATIONS, OR OTHER DATA ARE USED
FOR ANY PURPOSE OTHER THAN IN CONNECTION WITH A DEFINITELY
GOVERNMENT-RELATED PROCUREMENT, THE UNITED STATES GOVERNMENT INCURS
NO RESPONSIBILITY OR ANY OBLIGATION WHATSOEVER. THE FACT THAT THE
GOVERNMENT MAY HAVE FORMULATED OR IN ANY WAY SUPPLIED THE SAID
DRAWINGS, SPECIFICATIONS, OR OTHER DATA, IS NOT TO BE REGARDED BY
IMPLICATION, OR OTHERWISE IN ANY MANNER CONSTRUED, AS LICENSING THE
HOLDER, OR ANY OTHER PERSON OR CORPORATION; OR AS CONVEYING ANY
RIGHTS OR PERMISSION TO MANUFACTURE, USE, OR SELL ANY PATENTED
INVENTION THAT MAY IN ANY WAY BE RELATED THERETO.

THIS REPORT HAS BEEN REVIEWED BY THE OFFICE OF PUBLIC AFFAIRS
(ASD/PA) AND IS RELEASABLE TO THE NATIONAL TECHNICAL INFORMATION
SERVICE (NTIS). AT NTIS, IT WILL BE AVAILABLE TO THE GENERAL
PUBLIC INCLUDING FOREIGN NATIONS.

THIS TECHNICAL REPORT HAS BEEN REVIEWED AND IS APPROVED FOR
PUBLICATION.

R. C. EVERS
Polymer Branch
Nonmetallic Materials Division

T. E. HELMINIAK, Chief
Polymer Branch
Nonmetallic Materials Divison

FOR THE COMMANDER

MERRILL L. MINGES, Director
Nonmetallic Materials Divison

If your address has changed, if you wish to be removed from our
mailing list, or if the addressee is no longer employed by your
organization, please notify WRDC/MLBP, Wright-Patterson AFB, OH
45433-6533 to help us maintain a current mailing list.

Copies of this report should not be returned unless return is
required by security considerations, contractual obligations, or
notice on a specific document.

REPORT DOCUMENTATION PAGE

Form Approved
OMB No. 0704-0188

1a. REPORT SECURITY CLASSIFICATION Unclassified		1b. RESTRICTIVE MARKINGS		
2a. SECURITY CLASSIFICATION AUTHORITY		3. DISTRIBUTION/AVAILABILITY OF REPORT Approved for public release; distribution unlimited		
2b. DECLASSIFICATION/DOWNGRADING SCHEDULE				
4. PERFORMING ORGANIZATION REPORT NUMBER(S) WRDC--TR-90-4017		5. MONITORING ORGANIZATION REPORT NUMBER(S)		
6a. NAME OF PERFORMING ORGANIZATION Materials Lab WRDC, AFSC	6b. OFFICE SYMBOL *(If applicable)* WRDC/MLBP	7a. NAME OF MONITORING ORGANIZATION		
6c. ADDRESS *(City, State, and ZIP Code)* Wright-Patterson AFB, OH 45433-6533		7b. ADDRESS *(City, State, and ZIP Code)*		
8a. NAME OF FUNDING/SPONSORING ORGANIZATION Materials Lab, WRDC	8b. OFFICE SYMBOL *(If applicable)*	9. PROCUREMENT INSTRUMENT IDENTIFICATION NUMBER		
8c. ADDRESS *(City, State, and ZIP Code)*		10. SOURCE OF FUNDING NUMBERS		

8c. ADDRESS *(City, State, and ZIP Code)*	PROGRAM ELEMENT NO. 61102F	PROJECT NO. 2303	TASK NO. Q3	WORK UNIT ACCESSION NO. 07

11. TITLE *(Include Security Classification)*
Tenary Phase Diagrams of PBZT/Zytel 330/MSA and PBZT/Lubrizol/MSA Solutions

12. PERSONAL AUTHOR(S)
Charles Y-C Lee, Wansoo Huh, and S. J. Bai

13a. TYPE OF REPORT Final	13b. TIME COVERED FROM 8901 TO 8912	14. DATE OF REPORT *(Year, Month, Day)* 1990 January	15. PAGE COUNT 60

16. SUPPLEMENTARY NOTATION

17. COSATI CODES			18. SUBJECT TERMS *(Continue on reverse if necessary and identify by block number)*
FIELD	GROUP	SUB-GROUP	
07	04		
11	04		

19. ABSTRACT *(Continue on reverse if necessary and identify by block number)*
Effects of molecular interaction on rigid-rod/coil ternary systems were investigated in this report. The Ternary Phase Diagrams of PBZT/ZYTEL 330/MSA and PBZT/Lubrizol/MSA were determined and compared. The system with ZYTEL 330 showed phase behavior that agreed with Flory's Theory. The back-calculated aspect ratio of PBT decreased when "as-is" MSA was used instead of a CSA/MSA mixture. The Lubrizol system showed behavior that was not consistent with Flory's Theory. With Lubrizol, the concentration of PBT at critical concentration remained constant regardless of composition. The composition of the coagulated films was found to be influenced by solution composition, concentration, and states (isotropic vs anisotropic) of the solution.

20. DISTRIBUTION/AVAILABILITY OF ABSTRACT ☑ UNCLASSIFIED/UNLIMITED ☐ SAME AS RPT. ☐ DTIC USERS	21. ABSTRACT SECURITY CLASSIFICATION Unclassified	
22a. NAME OF RESPONSIBLE INDIVIDUAL Charles Y-C Lee	22b. TELEPHONE *(Include Area Code)* (513)255-9155	22c. OFFICE SYMBOL WRDC/MLBP

DD Form 1473, JUN 86   *Previous editions are obsolete.*   SECURITY CLASSIFICATION OF THIS PAGE

FOREWORD

This report was prepared by the Polymer Branch, Nonmetallic Materials Division. The work was initiated under Project No 2303, "Nonmetallic and Composite Materials," Task No 2303Q3, Work Unit Directive 2303Q307, "Structural Resin." It was administered under the direction of Materials Laboratory, Wright Research and Development Center, Air Force Systems Command, Wright-Patterson Air Force Base, Ohio, with Dr R. C. Evers as the Materials Laboratory Project Scientist. Co-authors were Charles Lee, Materials Laboratory (WRDC/MLBP), Wansoo Huh (Adtech Systems Research), and S. J. Bai (University of Dayton Research Institute). This report covers research conducted from June 1989 to Dec 1989.

TABLE OF CONTENTS

LIST OF FIGURES

Figure

LIST OF TABLES

Table

SECTION I

General Introduction

L. S. Tan, F. E. Arnold, and H. Chuah [1] reported the use of Lubrizol, a high molecular weight alkyl polymer with sulfonated side chains, in forming a molecular composite film with Poly[(benzo[1,2d:4,5d']bisthiazole-2,6-diyl)-1,4-phenylene (PBZT). This sytem represents a new class of rigid-rod molecular composite system that is different from all the rigid-rod molcular composite systems that were studies previously. All previous systems were systems where there were no interaction between the coil and the rigid-rod. The phase behavior of such systems was described by Flory's Theory which uses only volume exclusion consideration and does not assume any interaction between the rod and the coil. The Flory's theory was found to be in good agreement with experimental results of all the systems studied previously.

Because of the sulfonated side groups of Lubrizol, it serves as an ideal model compound to study the effect of coil-chain interaction on the ternary phase behavior. Specific interaction between the coil and the rod may give rise to unique properties in the molecular composites.

The ternary phase diagram of MSA/PBZT/Lubrizol was constructed in this study. The result showed that the behavior was different from that described by Flory's Theory. The reduced concentration of PBZT appeared to be a constant. This means that the PBZT is interacting with Lubrizol much the same way as the solvent molecule MSA. This interpretation is reasonable in considering that both MSA and Lubrizol have sulfonated groups in their structures. However, this behavior cannot be satisfactorily accounted for within the theoretical framework outlined by Flory. It is not clear whether the deviation was a breakdown of the Theory due to the presence of the coil/rod interaction or that the

1

interaction of the coil/solvent was such that the rod does not feel the presence of the coil. A phase diagram of MSA/PBZT/Nylon was also constructed by using the same molecular weight PBZT for comparison. The nylon system showed phase behavior that agreed with Flory's Theory. The back-calculated aspect ratio of PBZT decreased when "as-is" MSA was used instead of a CSA/MSA mixture.

Preliminary data were also included in this report on the coagulation of the ternary solution with water. The composition of the coagulated system appeared to be determined not only by the initial rod/coil composition, but also by the solution concentration as well. The role of the critical concentration on the coagulation behavior will be the subject of future studies.

SECTION II

Phase Diagram of PBZT/ZYTEL 330/MSA Solutions

2.1. INTRODUCTION

Continuous efforts to achieve practically useful molecular composite have been made in the Air Force Materials Laboratory since the first concept of molecular composite was reported more than ten years ago [2]. The molecular composite fiber of PBZT and ABPBI has been obtained and the uniaxial modulus of the composite exactly follows the general rule of mixture[3]. However, the preparation of high strength molecular composite of block has not been made successfully.

A processing method for making block molecular composite has been developed using methane sulfonic acid (MSA)[4]. The method is the direct block coagulation of the MSA solution under pressure followed by a consolidation step. As reported in previous technical reports of polybenzobisthiazole (PBZT) and nylon composite system [5-7], there exists a number of problems during the processing of block type composite, such as void formation during coagulation, phase separation of the second component, gellation phenomena, and the layer formation during consolidation step. The consequence of these problems leads to the poor mechanical properties of these final products. For this research, it is an attempt to understand the critical phase behavior of the ternary systems of Nylon/PBZT/MSA during the coagulation process.

3

2.2. EXPERIMENTAL

PBZT was prepared by SRI International in the form of a dope in polyphosphoric acid and these dopes were coagulated and pulverized into PBZT flakes by neutralizing and drying. The details of preparation procedure are well explained in the previous technical report[8]. The PBZT that was used in this study had an intrinsic viscosity of 16 dl/g (#A00131) in methane sulfonic acid(MSA) solution, corresponding to an average molecular weight of 27,000. Nylon components used as matrix were DuPont Zytel 330 (#A90720), which is amorphous polymer. All the polymers were used as received without further purification.

The ternary phase diagram of PBZT/Zytel 330/MSA system was studied in the range of the PBZT/Zytel 330 composition from 80/20 to 15/85. For a given PBZT/Zytel 330 composition, the critical concentration was determined by slowly titrating an anisotropic solution of known concentration until the solution becomes isotropic phase. The complete isotropic phases were confirmed by using optical microscopy under crossed polarizer. The weight fraction of polymers at the critical point was then calculated from the weight of solvent added. For each concentration, the stirring at room temperature usually lasted for three days in order to get a homogeneous solution. The same titration method was employed for the phase diagram of PBZT/Zytel 330 in mixed solvent of 97/3 composition of MSA/ chlorosulfonic acid (CSA).

The liquid crystalline phase was examined using Leitz Ortholux IIPOL-BK optical microscopy under crossed polarizer. By placing the PBZT/Zytel 330/MSA solution drop between two slide glasses and applying shear force, the anisotropic response under shear force was studied under crossed polarizer.

2.3. RESULTS AND DISCUSSION

2.3.1 FLORY'S THEORY

The Flory's theory [9] for the ternary system consisting of isodiameter solvent, random-coiled chain, and rigid-rod solute has been proposed to understand the critical phase behavior by assuming an "*athermal* condition", in which the free energy of mixing is zero. Due to the geometrical and molecular configuration difference between the rigid-rod and the flexible molecules, their compatibility during mixing is severely limited. Partitioning of solute components between nematic and isotropic phases in equilibrium is reminiscent of the fractionation of the pairs of rod-like solutes differing in axis ratio xi. The diameters of components rigid-rod and random-coiled chain are assumed equal to that of the solvent. The molecular volume of three components (solvent : rigid-rod: coil) are then in the ratio of 1: x_2 : x_3, where x_2 is the axis ratio of the rod molecule versus the solvent and similarly x_3 is that of the coil versus the solvent

Combinatorial analysis of the ternary system identified by use of the lattice model yields for the mixing partition function Z_M which implies the product of number of configuration of rodlike species and random coil molecules in the empty lattice. By utilizing Stirling's approximation for the factorials leads to the following Equation 1,

$$-\ln Z_M = n_1 \ln v_1 + n_2 \ln v_2 + n_3 \ln v_3 \quad n_0 \quad [\,1- v_2 (\ 1 - y/x_2)] \ln [1 - v_2 (\ 1 - y/x_2)] +$$
$$n_2 (y - 1) - n_2 \ln (x_2 y^2) + n_3(x_3 - 1) - n_3 \ln (x_3 z_3)] \tag{1}$$

where $n_0 = n_1 + n_2 x_2 + n_3 x_3$ (2)

where v_i is the volume fraction of respective components, z_3 is the internal configuration partition function for the random coil, y is the mean value of the disorder index at equilibrium. By making first differential of Equation 1 with respect to y, one obtains

5

$$\exp(-2/y) = 1 - v_2 \left(1 - y/x_2\right) \tag{3}$$

Substituting equation (3) into equation (1), the chemical potentials of the anisotropic phases can be derived

$$(\mu_1 - \mu_1^{\circ})/RT = \ln v_1 + v_2 (y - 1)/x_2 + v_3 (1 - 1/x_3) + 2/y \tag{4}$$

$$(\mu_2 - \mu_2^{\circ})/RT = \ln (v_2/x_2) + v_2 (y - 1) + v_3 x_2 (1 - 1/x_3) + 2(1 - \ln y) \tag{5}$$

$$(\mu_3 - \mu_3^{\circ})/RT = \ln (v_3/x_3) + v_2 (x_3/x_2) (y - 1) + v_3 (x_3 - 1) + 2 x_3/y - \ln z_3 \tag{6}$$

The chemical potentials in the isotropic phases are given as follows,

$$(\mu_1 - \mu_1^{\circ})/RT = \ln v_1 + v_2 (1 - 1/x_2) + v_3 (1 - 1/x_3) \tag{7}$$

$$(\mu_2 - \mu_2^{\circ})/RT = \ln (v_2/x_2) + v_2 (x_2 - 1) + v_3 x_2 (1 - 1/x_3) - \ln x_2^2 \tag{8}$$

$$(\mu_3 - \mu_3^{\circ})/RT = \ln (v_3/x_3) + v_2 x_3 (1 - 1/x_2) + v_3 (x_3 - 1) - \ln z_3 \tag{9}$$

At equilibrium between an isotropic phase and an anisotropic phase, one obtains by equating the chemical potentials given by Equations 4, 5, and 6 in the anisotropic phase (primed) to the corresponding chemical potentials in the isotropic phase (unprimed) given by Equations 7, 8, and 9, respectively.

$$\ln (v_1'/v_1) = A - B - 2/y \tag{10}$$

$$\ln (v_2'/v_2) = (A - B) x_2 - 2 \ln (x_2 e/y) \tag{11}$$

$$\ln (v_3'/v_3) = (A - B) x_3 - 2 x_3 /y \tag{12}$$

$$A = v_2 (1 - 1/x_2) + v_3 (1 - 1/x_3) \text{ and } B = v_2'(1 - 1/x_2) + v_3'(1 - 1/x_3) \tag{13}$$

6

Elimination of A - B by combination of Equations 12 with 11 gives

$$\ln(v_2'/v_2) - (x_2/x_3)\ln(v_3'/v_3) = 2\,x_2/y - 2\ln(x_2\,e/y) \qquad (14)$$

For given x_2, x_3, and v_2', these equations may be solved for y, v_3', and v_3 as follows. y can be obtained from Equation 3 with v_2 therein replaced by v_2'. Choice of trial values for v_2 and v_3 permits evaluation of A according to Equation 13 and of v_3' by use of Equation 14. Substitution of y, v_2', and v_3' in Equation 13 gives B value. Equation 11 may then be used to obtain a value for v_2 with which to replace the trial v_2. The value of v_2 that is consistent with the chosen v_2 may then be determined by iteration. Substitution of $v_1' = 1 - v_2' - v_3'$ in Equation 10 yields a value of v_1 which may be compared with $v_1 = 1 - v_2 - v_3$. A new value of v_3 may then be chosen and the procedure repeated and so forth until a satisfactory solution is obtained. The schematic diagram of whole calculation procedures using Flory's theory is shown in Figure 1.

Figure 2 shows the theoretical treatment of critical concentration calculated using different aspect ratio of rigid molecules and the contour length of coil-like molecules. It can be seen that for a given set of x_2 and x_3, the phase segregation phenomena is enhanced with increase of rod length, x_2, and the critical concentration occurs at lower concentration. And, as more flexible molecules are introduced, the volume available for rod-like polymers decreases and so that the rodlike polymers are more packed and aligned in the anisotropic phase. However, the effect of the chain length of the flexible coil polymer, x_2, on the phase diagram is not so marked as the effect of rigid-rod polymer. This suggests that the dominant factors in constructing phase diagram are the axis ratio of rigid molecules and the composition ratio of rigid polymer and coil polymer.
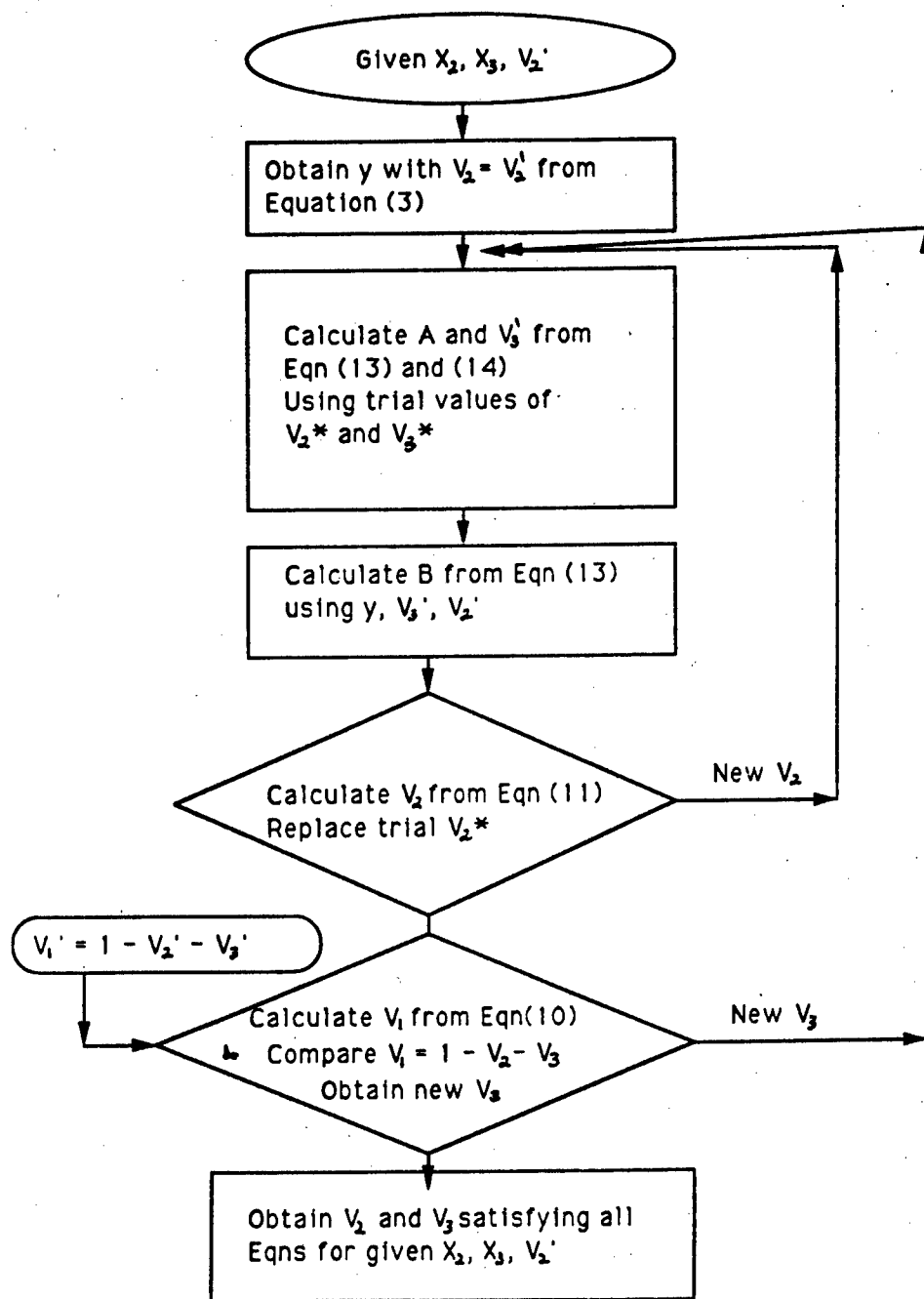
Figure 1. Schematic Diagram of Flory's Calculation for Ternary System

The flowchart contains the following elements:

- Given X_2, X_3, V_2'
- Obtain y with $V_2 = V_2'$ from Equation (3)
- Calculate A and V_3' from Eqn (13) and (14) Using trial values of V_2* and V_3*
- Calculate B from Eqn (13) using y, V_3', V_2'
- Calculate V_2 from Eqn (11) Replace trial V_2* — New V_2
- $V_1' = 1 - V_2' - V_3'$
- Calculate V_1 from Eqn(10) Compare $V_1 = 1 - V_2 - V_3$ Obtain new V_3 — New V_3
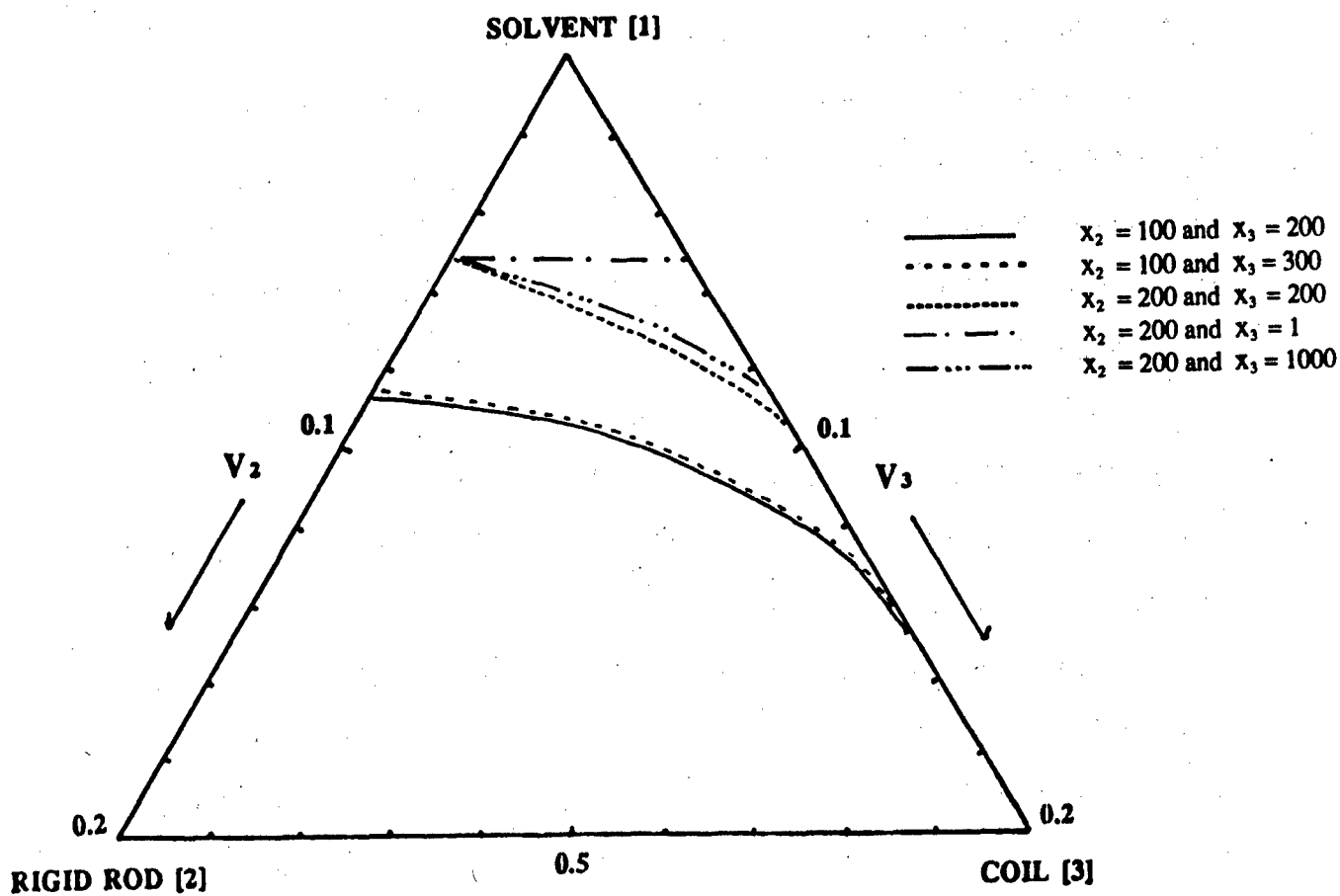- Obtain V_2 and V_3 satisfying all Eqns for given X_2, X_3, V_2'

Figure 2. Theoretical Treatment of Critical Behavior of Rigid-Rod/Coil/Solvent System
Using Different Aspect Ratio of Rigid-Rod, x_2 and Contour Length of Coil, x_3

9

2.3.2. PHASE DIAGRAM OF TERNARY SYSTEM

The theory recently developed by Flory [9] described the critical phase behavior of a ternary system consisting of isodiametrical solvent, rigid-rod polymer, and flexible coil polymer. This theoretical analysis can be directly applied to the experimental result. With the mixed solvent of 97/3 wt. % ratio of MSA/CSA, the critical behavior of PBZT/Zytel 330/solvent system was studied and is shown in Figure 3. The experimental critical concentrations are summarized and compared with the theoretically calculated values in Table 1. The theoretical aspect ratio of PBZT molecules are estimated to be 256 from the model compound of repeat unit length of 12.2 A, repeat unit width of 4.691 A, and polymer molecular weight of 27,000. The contour length of 300 for the Nylon flexible polymer was adopted for the theoretical calculation[10]. As seen in Figure 3 and Table 1, the experimental results for PBZT/Zytel 330/MSA-CSA system are in excellent agreement with the theoretically predicted values.

The same phase diagram was constructed for PBZT/Zytel 330/MSA system and shown in Figure 4. The MSA used was 99 % MSA "as is" from Aldrich Chemicals without distillation. By titrating the anisotropic solutions of 100/0, 70/30, 50/50, 30/70, 15/85, 5/95 PBZT/Zytel 330 blends, all the critical concentrations were determined. They are 4.0 %, 4.4 %, 4.8 %, 5.3 %, 5.8 %, 6.6 % respectively. With decreasing amount of rigid-rod PBZT polymer, the trend of increasing critical concentration can be observed as predicted by Flory's theory. When compared with the PBZT/Zytel 330/MSA-CSA critical phase boundary as shown in Figure 3, some discrepancy of critical behavior can be found. It is due to the presence of small amounts of moisture in MSA solvent, which results in the aggregation of PBZT molecules[11]. The effect of the aggregation is a decrease of actual aspect ratio of rigid molecules in the solution. Using the "as is" MSA phase diagram to
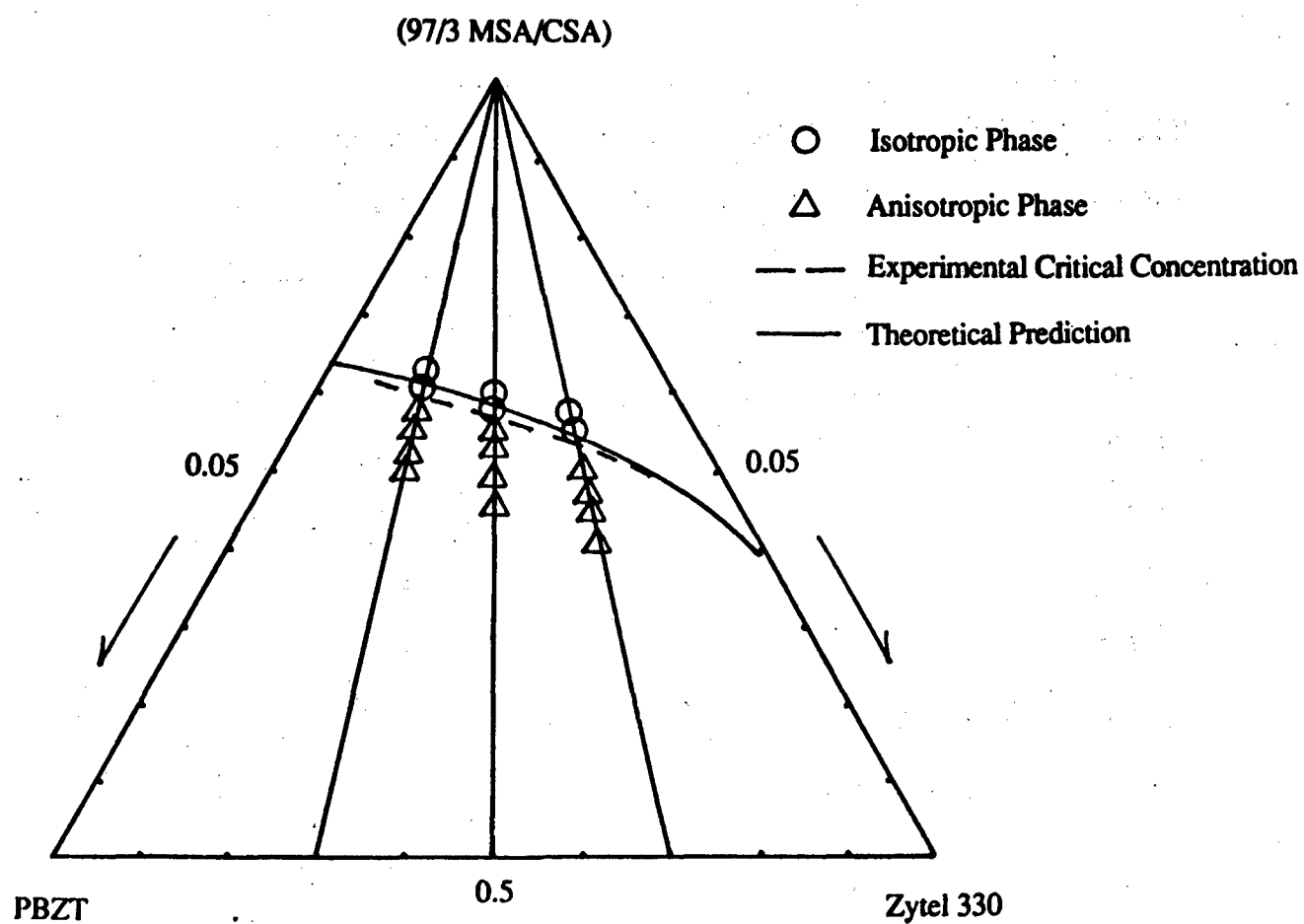
10

Figure 3. Experimental Phase Diagram of PBZT/Zytel 330/MSA-CSA System

TABLE 1. Critical Phase Concentration of PBZT/Lubrizol/MSA

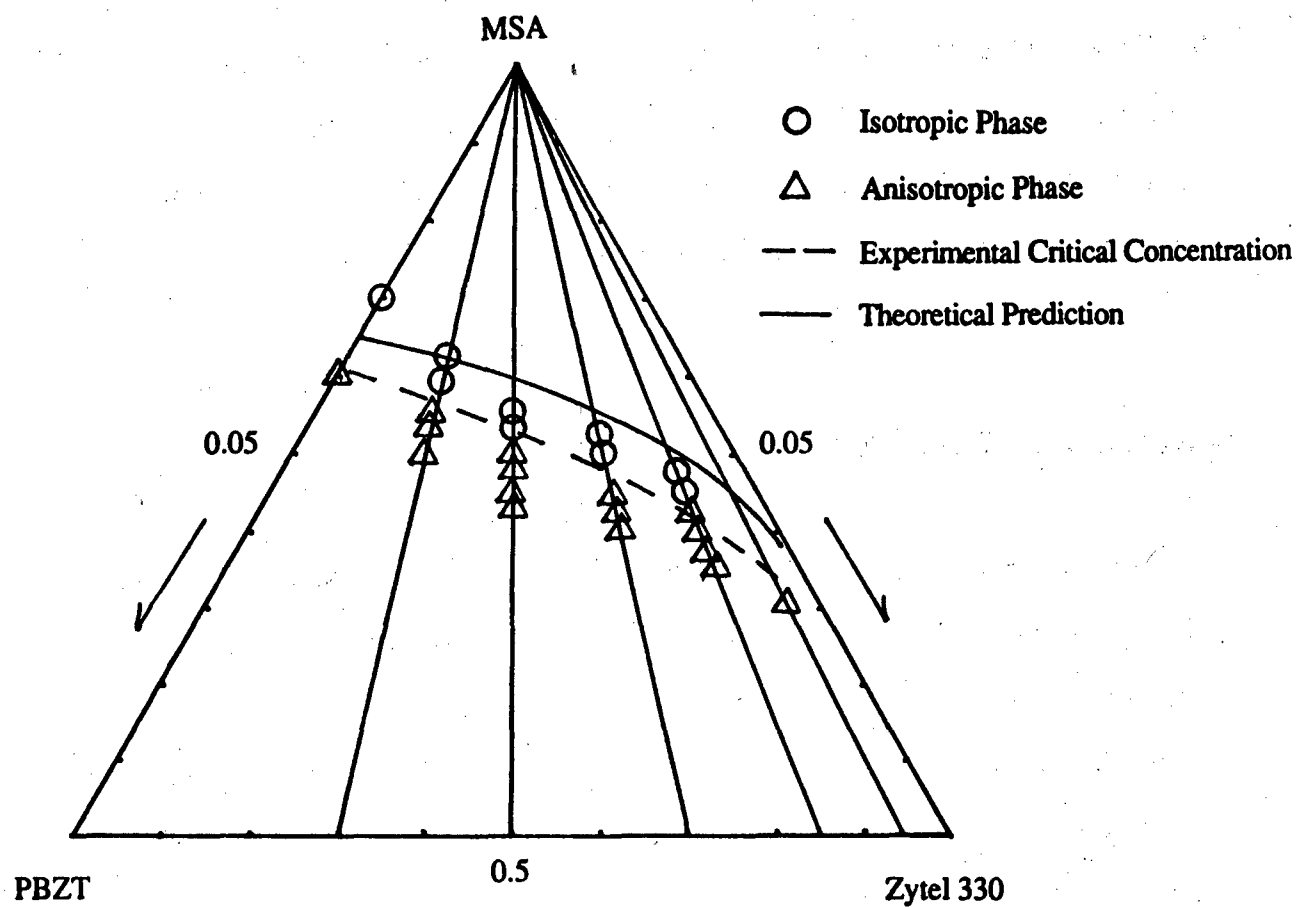| PBZT/ZYTEL 330 Composition	C_{Cr} in MSA (wt. %)	C_{Cr} in 97/3 MSA/CSA (wt.%)	Calculated C_{Cr} (wt. %)
100/0	4.0	***	3.6
70/30	4.4	4.0	3.9
50/50	4.8	4.3	4.2
30/70	5.3	4.7	4.5
15/85	5.8	***	4.9

Figure 4. Experimental Phase Diagram of PBZT/Zytel 330/MSA System

backcalculate the aspect ratio of the rigid molecules, the data showed a value of 220, a

decrease by 14 %. Using the Halpin-Tsai Equation, this will only have a minimum effect

on the reinforcing efficiency. So using the "as is" MSA would be acceptable for the

practical applications. But using "as is" MSA also means that a certain degree of PBZT

aggregation exists in the solution before coagulation[4]. Therefore, it is not surprising that

WAXD result of consolidated block showed the evidence of aggregation of rigid-rod

molecules. It is not clear whether additional aggregation is generated during the

coagulation process, and further decreases the aspect ratio of the reinforcement entities,

compromising the reinforcement efficiency of the rigid -rod molecules.

2.3.3 OPTICAL MICROSCOPY

The anisotropic solution of 5.8 wt% 5/5 PBZT/Zytel 330 in MSA was examined

using optical microscopy under crossed polarizer. The solution is above the critical

concentration(4.8 wt%) and optically opaque and shows dark green color. As seen in

Figure 5-a, the liquid crystalline domains can be observed. With application of shear force,

the anisotropic shear band can be found perpendicular to the shear direction mixed with

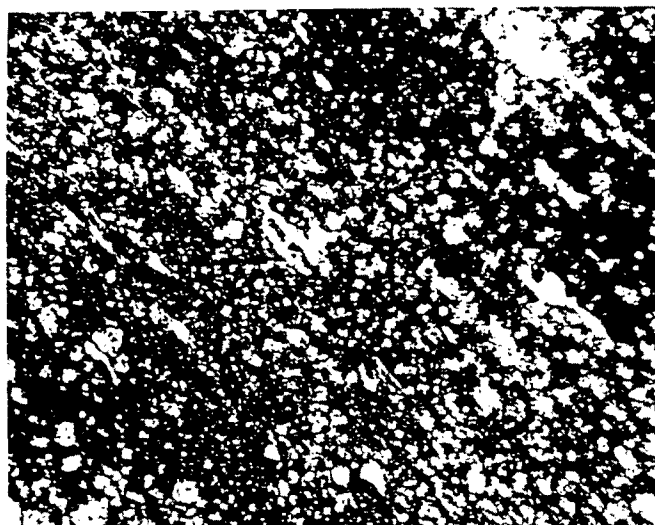isotropic dark region (Figure 5-b).

a).
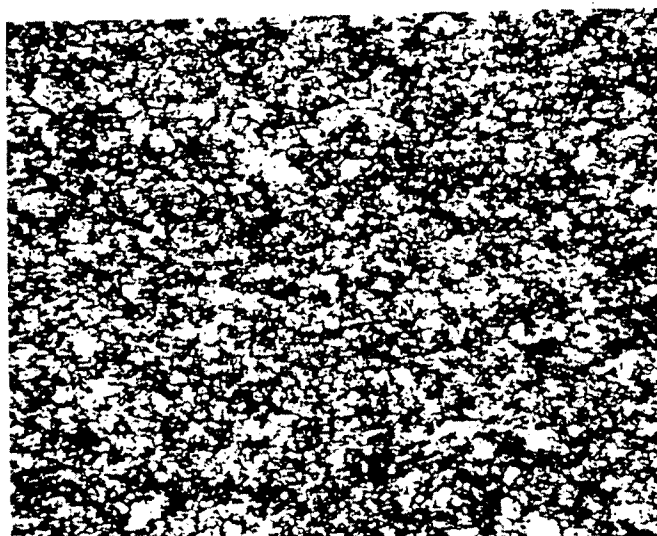
b).

Figure 5. Optical Microscopy of 5.8% 50/50 PBZT/Zytel 330 in MSA;

a) no shear force and b) shear force applied

SECTION III

## Phase Transition of PBZT/Lubrizol Solution

3.1 INTRODUCTION

A ternary system of rigid-rod/coil/solvent was investigated for its nematic to
isotropic phase transition behavior. The rigid-rod component was PBZT which had a para-
catenated backbone leading to a rodlike polymer [12]; its chemical structure is sketched in
Figure 6-a. PBZT is a high-temperature polymer with no glass transition behavior up to
decomposition temperature and is soluble only in strong acids, such as methanesulfonic
acid (MSA). In solution, PBZT exhibits lyotropic liquid-crystalline characteristics, i.e.
below a critical concentration C_{Cr} the morphology changed from anisotropic (nematic) to
isotropic. PBZT used in this study had an intrinsic viscosity of 16 dl/gm as determined in
MSA at 30 °C. Lubrizol, poly(sodium 2-acrylamido-2methylpropanesulfonate) as shown in
Figure 6-b, is a large linear polymer (with molecular weight about 3-4 x 10^6) soluble in
MSA and H_2O, and is known to degrade for long-term exposure in acid based on a
decrease of 15 percent in inherent viscosity over a period of two weeks in MSA [13]. In
having a sulfonate moiety on each side chain, Lubrizol is deemed to have certain
protonation interaction with PBZT. The effect of this interaction in the ternary solution of
PBZT/Lubrizol/MSA was examined by C_{Cr} determination.

3.2 EXPERIMENTALS

PBZT involved in this study was coagulated in H_2O, from polymerization dope.
The dried and powderized PBZT was used for making the composite solutions. "Lubrizol
2420" as received, was a milky white, viscous, aqueous liquid. It was precipitated into a

16

. Poly(para-phenylene benzobisthiazole) (PBZT)
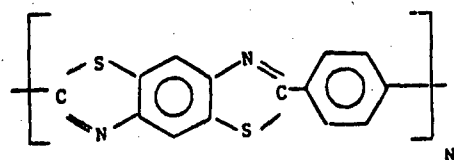
. Poly(sodium 2-acrylamido-2-methylpropanesulfonate) Lubrizol
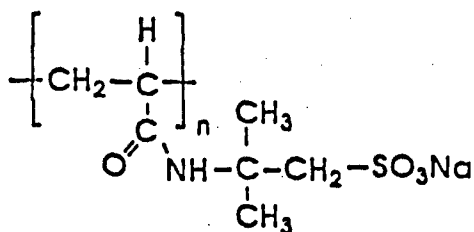
Figure 6. a) Chemical Structure of poly(p-phenylene benzobisthiazole)(PBZT)

and b) Chemical Structure of Lubrizol

mixture of toluene and methanol resulting in wax like polymer. After filtering and washing, the Lubrizol polymer was dried and made into powder [13].

Various compositions of PBZT/Lubrizol were codissolved in distilled MSA for forming homogeneous solutions. The compositions were 100/0, 70/30, 50/50, 40/60, 20/80 and 0/100 for PBZT/Lubrizol weight ratio. The solutions could be either isotropic or anisotropic (nematic) depending on the polymer concentration. The phase transition was induced by changing the polymer concentration either by titration, or by adding polymers while maintaining the rigid-rod/coil composition. As the polymer concentration approaches the phase transition concentration (C_{Cr}), there was a significant increase in solution viscosity making mechanical stirring for a homogeneous solution ineffective. We circumvented this difficulty by manually stirring a small amount of the solution. This greatly facilitated the preparation of homogeneous solutions required for phase transition study.

C_{Cr} of the homogeneous solution was determined by examining the solution morphology using optical microscopy. In the nematic phase, the aggregation of the rod-like PBZT polymer constitutes anisotropic domains; each with the PBZT polymer aligned along a director which was usually the long-axis of the domain. While a polarized white light passing through the anisotropic medium, it would induce birefringence showing different colors according to the director orientation. For an isotropic solution which does not have the aggregation of the rod-like PBZT polymer, this disperse chromatic effect would not be observed. Instead, the solution would be monochromatic under cross polar light.

In addition, complementary observations on viscosity and stir opalescence of the solutions proved to be very helpful in determining C_{Cr} for each composition. According to Flory's [14] and Onsager's [15] theories, while the rigid-rod polymer concentration increased to C_{Cr}, the viscosity of the solution would raise significantly, and under a shear

18

field the translucent isotropic solution will become opaque, this is called stir-opalescence. As the polymer concentration increases further toward C_{Cr}, the solution viscosity will increase accordingly (making it difficult to be homogeneous) and the stir-opalescence becomes more persistent. As the polymer concentration increased beyond C_{Cr}, the biphasic morphology remains, the viscosity decreases and the opalescence is always present. To the contrary, an isotropic liquid-crystalline polymer solution displays no birefringence under cross polar, no persistent stir-opalescence, and lower viscosity. C_{Cr} of a homogeneous solution is defined as the concentration at which the isotropic solution becomes biphasic with optically anisotropic domains dispersed in an isotropic background, or the biphasic solution becomes isotropic with optically anisotropic domains disappeared forming an isotropic solution, which both can be observed by optical microscopy.

The solution containing a lyotropic liquid-crystalline polymer undergoes a nematic to isotropic phase transition over a very small range of concentration. For this reason, it was difficult to determine precisely a critical concentration and the changes in polymer concentration were kept small to avoid overshooting the phase transition. We examined our solutions using optical microscopy for C_{Cr} at which the solution changed from biphasic to isotropic, or vice versa, under cross-polar. For selected compositions of 100/0, 70/30, 50/50, 40/60, 20/80 and 0/100 PBZT/Lubrizol weight ratio, homogeneous solutions were obtained and examined as aforementioned.

3.3 RESULTS AND DISCUSSION

Since Lubrizol is not stable in MSA and also for demonstrating reproducibility, the experiment was repeated for each composition with narrower concentration range and thus less time consuming and less acid degradation to Lubrizol. This repetition produced similar C_{Cr}; the effect of acid degradation of Lubrizol on C_{Cr} of the ternary solutions was negligible.

For example, the largest discrepancy was observed for the 50/50 PBZT/Lubrizol composite solutions. After many changes of polymer concentration during a period over one month, the first composite solution showed a C_{Cr} of 6.60%. The second solution started as an isotropic solution and reached the biphasic state quickly showing a C_{Cr} of 6.96%. We adopt the latter value of C_{Cr} as the critical concentration for this ternary solution for expecting much less acid degradation happened to the Lubrizol. Similar procedure was applied for other compositions revealing even more self-consistent C_{Cr} values. The result of C_{Cr} determination is shown as a ternary phase diagram in Figure 7 for the ternary solutions.

For providing base data, two PBZT in MSA (100/0) solutions was prepared and observed to be biphasic at 3.65% and 3.66% weight fraction. Its C_{Cr} is estimated to be between 3.60% and 3.70% and a value of 3.65% is adopted. Taking into account the PBZT intrinsic viscosity, the aspect ratio of the rigid-rod is estimated to be 240. [16] For this composition, the Lubrizol concentration is zero. The classical theory on rigid-rod phase transition [14] is applicable here and gives a C_{Cr} of 3.6%. This result is remarkably close to the experimental C_{Cr} considering the *athermal* assumption involved in the theory [14]. Similar effort was spent on the study of pure Lubrizol in MSA solution (0/100) not for nematic to isotropic phase transition behavior but for solubility and acid stability. At about 7% weight fraction, a gelation behavior was observed for Lubrizol in MSA. After an effort over a period of about two weeks, the Lubrizol concentration was increased
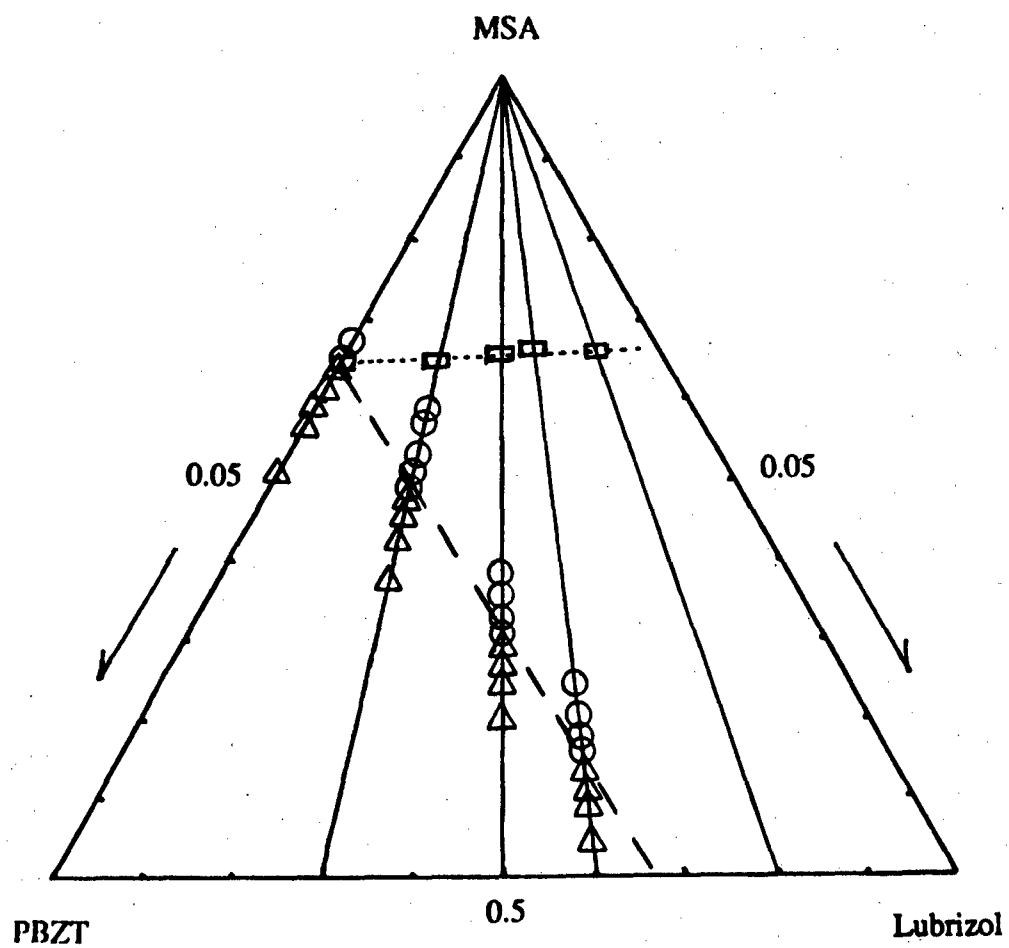
Figure 7. Phase Diagram of PBZT/Lubrizol/MSA System

gradually to about 25% for a homogeneous solution. Its gelation behavior still persisted without abating from acid degradation.

There are possibly two kinds of protonation interaction involving PBZT in the ternary system: PBZT with MSA and PBZT with Lubrizol. Over a wide composition range the ternary phase diagram does not show any distinction between these two. Instead, the linear relationship shown in the phase diagram seems to suggest that Lubrizol has behaved exactly like MSA in the ternary solution. The effect from a long coil-like Lubrizol polymer is not evidenced. Table 2 compiles C_{Cr} for each composition together with reduced PBZT concentration at C_{Cr}. It is obvious that the reduced PBZT concentration at C_{Cr} is a constant independent of Lubrizol content and agrees with that of pure PBZT in MSA.

Considering the ternary phase equilibrium theory proposed by Flory [9], the effective molar volume ratio x_3 for the Lubrizol in the ternary solution would be one just like that of the MSA solution. This is a surprising result in view of Lubrizol is a linear polymer with very high molecular weight; its x_3 should have been in the order of 10^3 - 10^4 leading to a much lower C_{Cr} for the ternary solution. However, the effect of protonation interaction between PBZT and Lubrizol might have a role here. The stochiometric molar ratio for the protonation interaction is 33/67, or a weight ratio of 32/68, for PBZT/Lubrizol. For the compositions of 100/0, 70/30, 50/50 and 40/60, the protonation interaction of the PBZT molecule in the ternary solution can not be totally attributed to the Lubrizol. Nevertheless, these composite solutions show a similar reduced PBZT concentration at C_{Cr} like that of the 20/80 composite solution which is possible fully protonated by the Lubrizol. In addition, the Lubrizol gelled at about seven weight percent in MSA. In the 20/80 composition solution, which contained about 13 weight percent of the Lubrizol, the gelation phenomenon was observed during solution preparation. An identical reduced PBZT concentration at C_{Cr} was obtained suggesting the gelation of Lubrizol had no effect in the phase behavior of the ternary system. Finally, the Flory's modified lattice theory does take into account the excluded volume effect but not, by assuming *athermal*, the

TABLE 2 Critical Concentration of PBZT/Lubrizol/MSA System

PBZT/Lubrizol Composition	Ccr(wt.%)	Reduced PBZT Conc.(wt.%)
100/0	3.65	3.65
70/30	5.14	3.59
50/50	6.96	3.48
40/60	8.25	3.30
20/80	16.92	3.38

mixing free energy or intermolecular interaction. The excess protonation interaction between PBZT and Lubrizol polymer seems to balance the excluded volume effect from chain configuration of, and the gelation behavior of the large molecule Lubrizol giving a x_3 value of one. By which, it is a very intriguing experimental result.

SECTION IV

Coagulation of PBZT/Lubrizol Blends

4.1 INTRODUCTION

Because of its rigid chain configuration, the rigid-rod heterocyclic aromatic family (poly-p-phenylene benzobisthiazole (PBZT), poly-p-phenylene benzobisoxazole (PBO) etc.) has been studied extensively in the past for their unusual mechanical properties. As a single component, the polymers can be processed into high performance fibers. The polymers can also be used as reinforcement entities when they are dispersed in other polymers to form structural molecular composites. Because of their conjugated structures, these polymers and the related ladder polymers were found to possess other interesting properties like conductivity [17] and non-linear optics responses [18]. These types of polymers would be an ideal polymer to investigate multi-functional materials.

For all the molecular composite systems investigated in the past, the rigid-rod molecules and the coil molecules were codissolved in methane sulfonic acid (MSA) to form a three component solution which was subsequently processed to form a two components molecular composite. The ternary phase diagram of the three components solution was described by the Flory's theory [9] which is based upon the topological difference (rigid-rod and flexible coil) of the two polymers and does not contain any description of specific interactions between them. However, specific interaction may be desirable in forming multi-functional materials. This study is to investigate the effect of specific interaction between the rod and the coil polymers on the ternary phase diagram and the coagulation behavior of the two-component molecular composite.

4.2 EXPERIMENTALS

A ternary system of rigid-rod/coil/solvent was investigated for its nematic to isotropic phase transition behavior. The rigid-rod component is poly-p-phenylene-benzobisthiazole (PBZT) which has a para-catenated backbone leading to a rodlike polymer; its chemical structure is sketched in Figure 6-a. In solution, PBZT exhibits lyotropic liquid-crystalline characteristics, i.e. below a critical concentration C_{Cr} the morphology changed from anisotropic (nematic) to isotropic. PBZT used in this study had an intrinsic viscosity of 16 dl/gm (#A00131) as determined in MSA at 30 °C. Lubrizol, poly(sodium 2-acrylamido-2-methylpropanesulfonate) as shown in Figure 6-b, is a large linear polymer (with molecular weight about 3-4 x 10^6) soluble in MSA and H_2O, but will degrade for long-term exposure in acid as evidenced by the decrease in specific viscosity as a function of time [13]. In having a sulfonate moiety on each side chain, it is possible for Lubrizol^{TM} to have protonation interaction with PBZT.

For the coagulation behavior analysis, six different solutions, 5.5 % 50/50 PBZT/Lubrizol, 7.6 % 50/50 PBZT/Lubrizol, 4.0% 70/30 PBZT/Lubrizol, 5.44% 70/30 PBZT/Lubrizol, 5.6% 30/70 PBZT/Lubrizol, and 9.9 % 30/70 PBZT/Lubrizol mixtures in MSA solvent, were prepared. The mixing of these solutions continued for 6-7 days until the completely homogeneous solutions were obtained. Thin films from these solutions were prepared on glass slides using a doctor blade. By placing 30-40 ml of solution on a glass slide and applying the shear force with doctor blade, the very thin smeared solution films were prepared on the glass slide. The prepared solution films were immediately coagulated in the distilled water for 24 hours. The wet coagulated films were vacuum-dried between two teflon plates under pressure for 1-2 days at 110 °C. The composition variation of PBZT and Lubrizol in the coagulated films was studied using a Beckman infrared spectrometer FT-1100.

26

For the rheological measurements of Lubrizol component in MSA, the viscosity of Lubrizol/MSA system has been investigated using Rheometrics Mechanical Spectrometer (RMS) with parallel plates at room temperature. For the Lubrizol concentrations ranging from 1 to 14 wt.%, the steady shear viscosity at zero shear rate region was obtained.

WAXD was used to study the aggregation PBZT molecules and phase separation of PBZT/Lubrizol coagulated blends. WAXD patterns were recorded with a flat-film Statton (Warhus) camera using Cu Kα radiation, with a Ni filter, and a sample-to-filter distance of 5 cm.

4.3   RESULTS AND DISCUSSION

4.3.1.   FTIR

For the molecular composite, it is desirable to have a molecular morphology in which the rigid molecules are evenly dispersed in the coil-like polymer. This can be easily obtained by using a common solvent in the isotropic state just below the critical concentration. During the processing to solid state, the thermodynamic phase separation between rigid-rod and flexible molecules is inevitable and this can only be prevented by using kinetic approach, quickly transfering the isotropic solution to the coagulant and preserving the isotropic solution morphology in the solid state. However, it is not clear whether real molecular level composite was obtained without phase separation through the coagulation process. Therefore, by utilizing the Lubrizol polymer which could offer the ionic interaction with PBZT molecules and studying the coagulation behavior of PBZT/Lubrizol/MSA system, the effect of ionic interaction during the coagulation process was studied. The composition ratio of PBZT and Lubrizol components before and after coagulation procedure was analyzed using FTIR and TGA analysis. Since the Lubrizol is soluble in water, the coagulated composition of PBZT/Lubrizol blend should be different

27

depending upon the initial solution morphology and coagulation stage. Also, the effect of critical concentration on the coagulation composition was studied.

Figure 8 shows the FTIR spectrum of pure Lubrizol powder mixed with KBr pellet. The characteristic spectra of Lubrizol component can be observed at 1673.5 cm^{-1} which is believed to be the carbonyl stretching. In Figure 9, the spectrum of pure PBZT powder is shown. The C=N stretching can be found at 1483.6 cm^{-1} and PBZT component shows a very strong absorption band at 959.1 cm^{-1} which is assigned to the C - S bond in PBZT component by using the IR table in reference[19]. Therefore, the unique chemical structure of PBZT and Lubrizol component to be useful for the analysis of coagulation composition in FTIR spectrum are carbon-sulfur group at 959.1 cm^{-1} and C=O group at 1673.5 cm^{-1} respectively. By using these two IR spectra and measuring the areas of two peaks, the composition analysis of the two components in the coagulated blends was made.

According to Beer-Lambert law, the absorbed radiation should be equal to the product of concentration c, path length of the beam through the sample db, and the amount of radiation per square centimeter, I. In Equations form, this can be summarized by,

$$-dI = a' \, c \, I \, db \qquad (15)$$

$$\log_{10} (I/I_0) = \log T = - a \, b \, c \qquad (16)$$

$$A = a \, b \, c \qquad (17)$$

where a' is a proportionality factor whose value depends on the absorbing molecules at a particular frequency. Through the integration of Equation (15), Beer-Lambert law can be expressed using percent transmission T and absorptivity a. By converting the percent transmission to absorbance A, the Equation (17) which can be useful for IR analysis, is obtained. Since the absorbance A is directly proportional to the spectrum absorbance area,
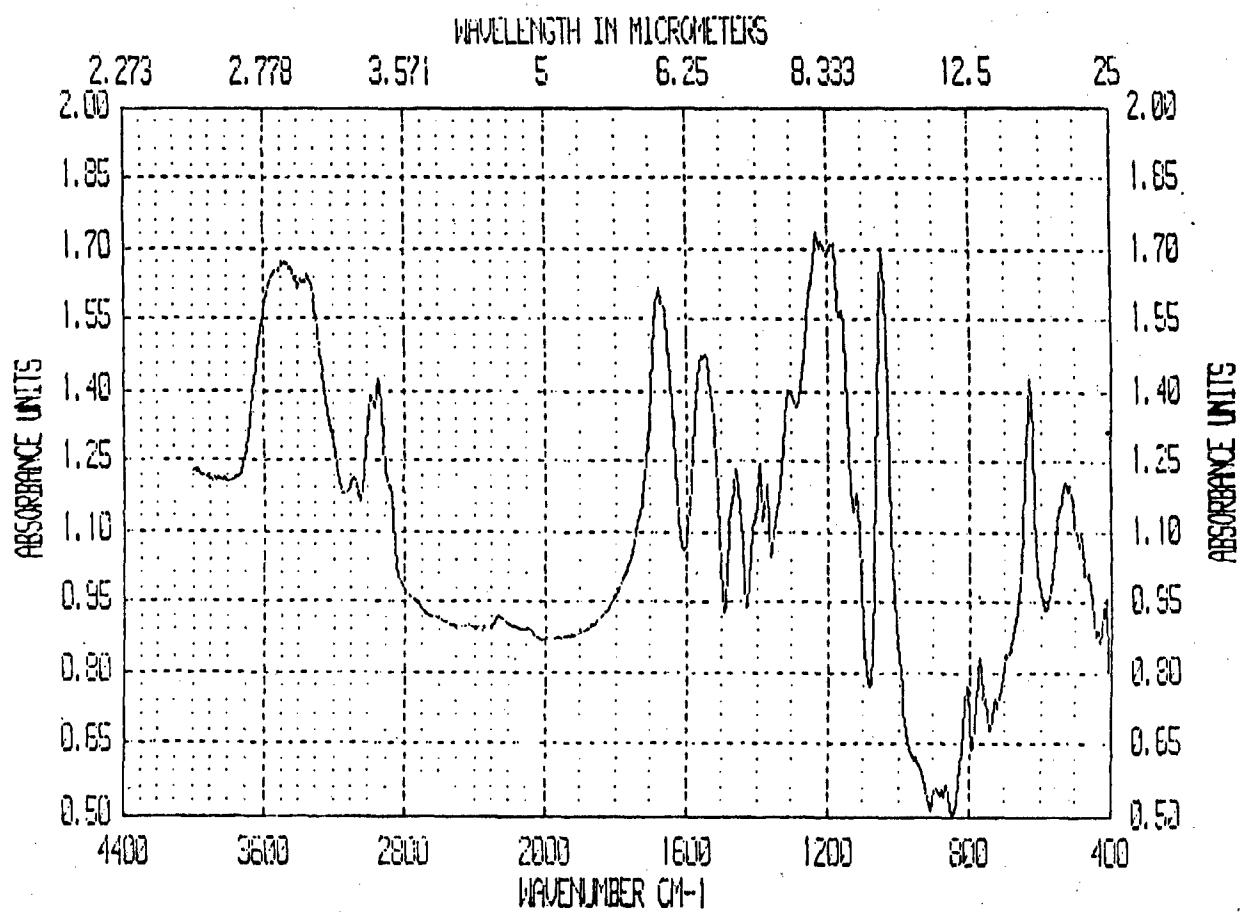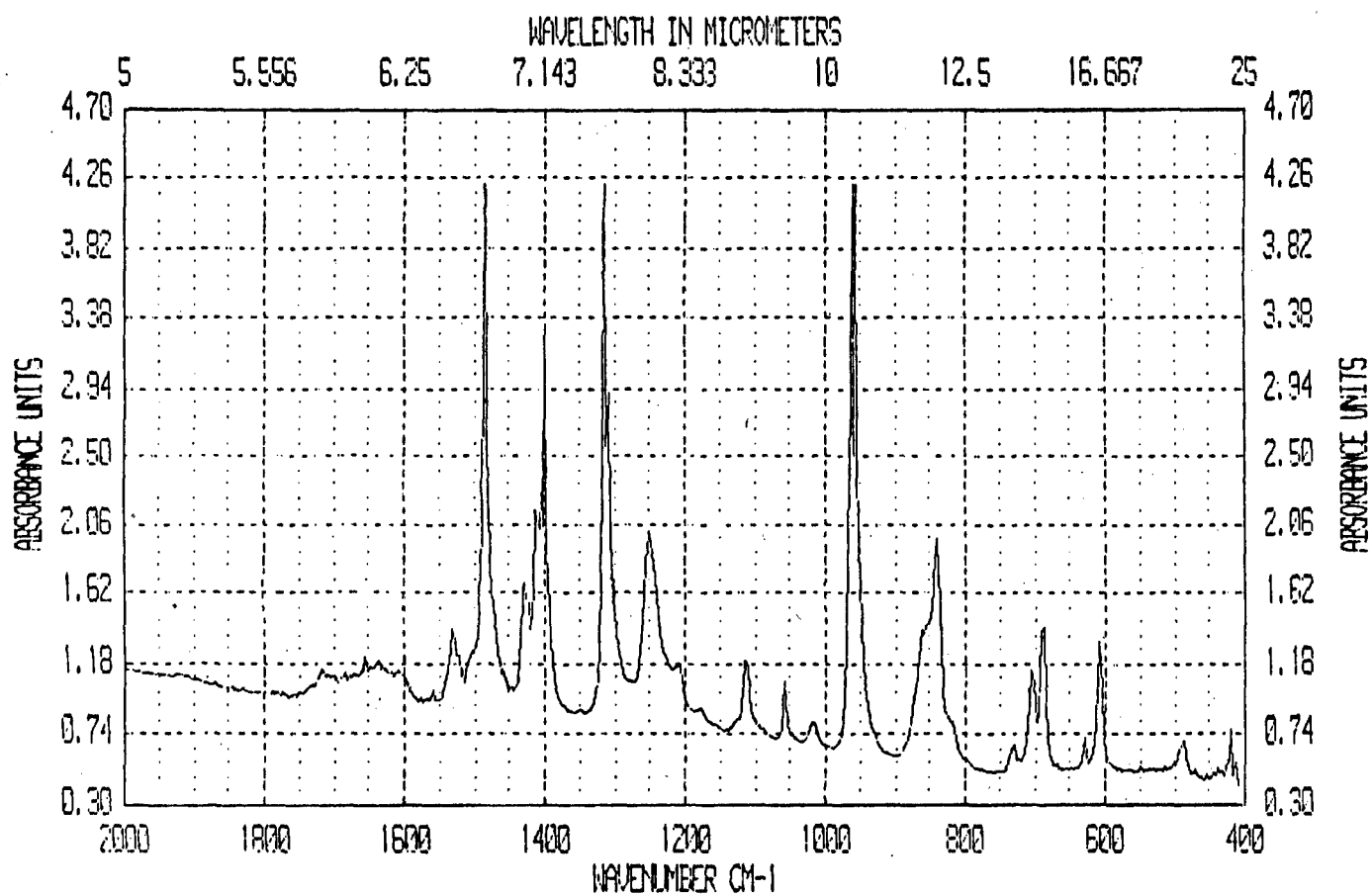
Figure 8. FTIR Spectrum of Lubrizol

Figure 9. FTIR Spectrum of PBZT

the composition ratio of the PBZT/Lubrizol blend can be calculated using characteristic

spectra of PBZT and Lubrizol respectively. When each area of the two absorption bands

at 1673.5 cm^{-1} and 959.1 cm^{-1} were measured from the base line, the absorbance of each

spectra can be expressed using Beer-Lambert law. The ratio of two absorbances in the

blend is shown in Equation (18), since the segmental lengths, b_1 and b_2, are the same.

$$A_1/A_2 = a_1\, b_1\, c_1\, /\, a_2\, b_2\, c_2 = a_1\, c_1\, /\, a_2\, c_2 \qquad (18)$$

From the IR spectra of reference mixtures of known composition ratio, it is

possible to obtain the ratio of $a_1 c_1 / a_2 c_2$ using Equation (18). For this study, three

reference samples were prepared by mixing the powder of 30/70, 50/50, and 70/30

PBZT/Lubrizol composition. Using Equation (18), the characteristic calibration curve of

PBZT/Lubrizol system can be constructed by calculating the ratio of $a_1 c_1 / a_2 c_2$ as a

function of composition. Figure 10 exhibits the calibration curve of PBZT/Lubrizol

mixture and from this figure, the composition ratio of PBZT/Lubrizol blend with unknown

composition can be calculated. The infrared spectra of these reference samples are shown

in Appendix I. In order to check the linearity of above the relationship, the intensity ratio

of A_2/A_1 as a function of $MW_1\, wt_2 / MW_2\, wt_1$ was plotted and shown in Figure 11.

The almost perfect straight line of Figure 11 suggests that the calibration curve in Figure 10

is valid within the composition range studied.

Coagulated films of 7.6 % 50/50 PBZT/Lubrizol, 5.5% 50/50 PBZT/Lubrizol,

4.0% 70/30 PBZT/Lubrizol, 5.44% 70/30 PBZT/Lubrizol, 5.6% 30/70 PBZT/Lubrizol,

and 9.9 % 30/70 PBZT/Lubrizol compositions were investigated using FTIR analysis. The

IR spectra of these blends are shown in Appendix II. In Figure 12, the IR spectra of

different PBZT/Lubrizol composition at 1673.5 cm^{-1} and 959.1 cm^{-1} are shown. With

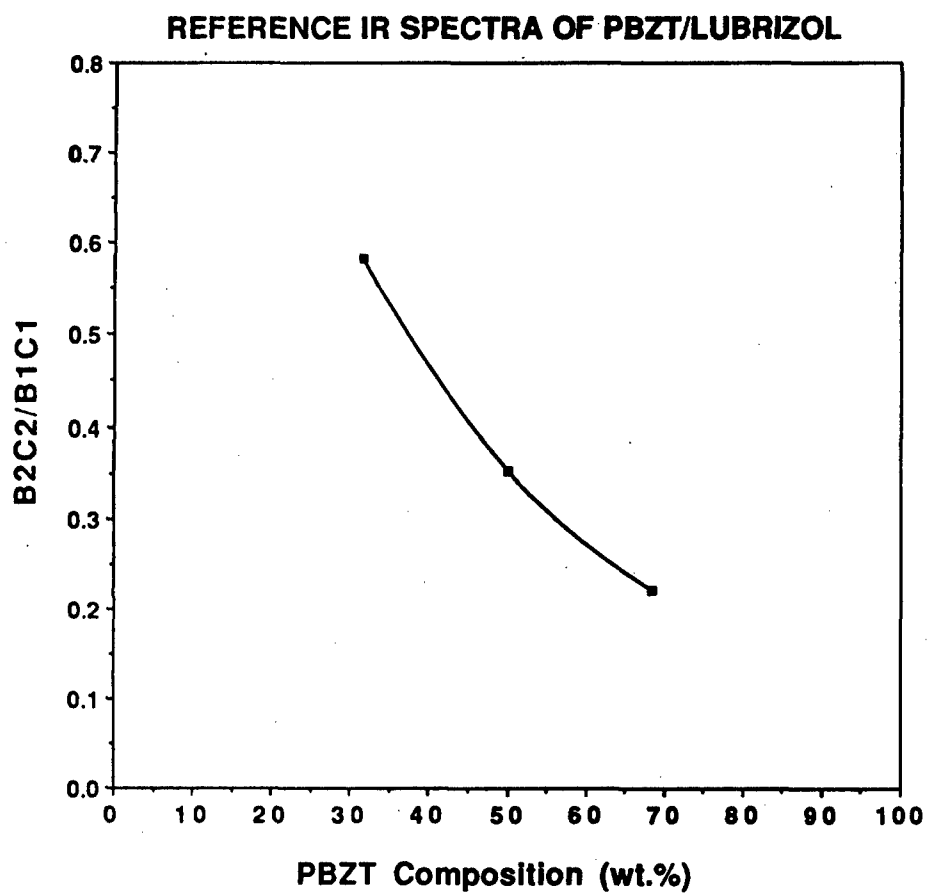increasing PBZT content from 30 % to 70 % in PBZT/Lubrizol mixture, the carbonyl

31

REFERENCE IR SPECTRA OF PBZT/LUBRIZOL

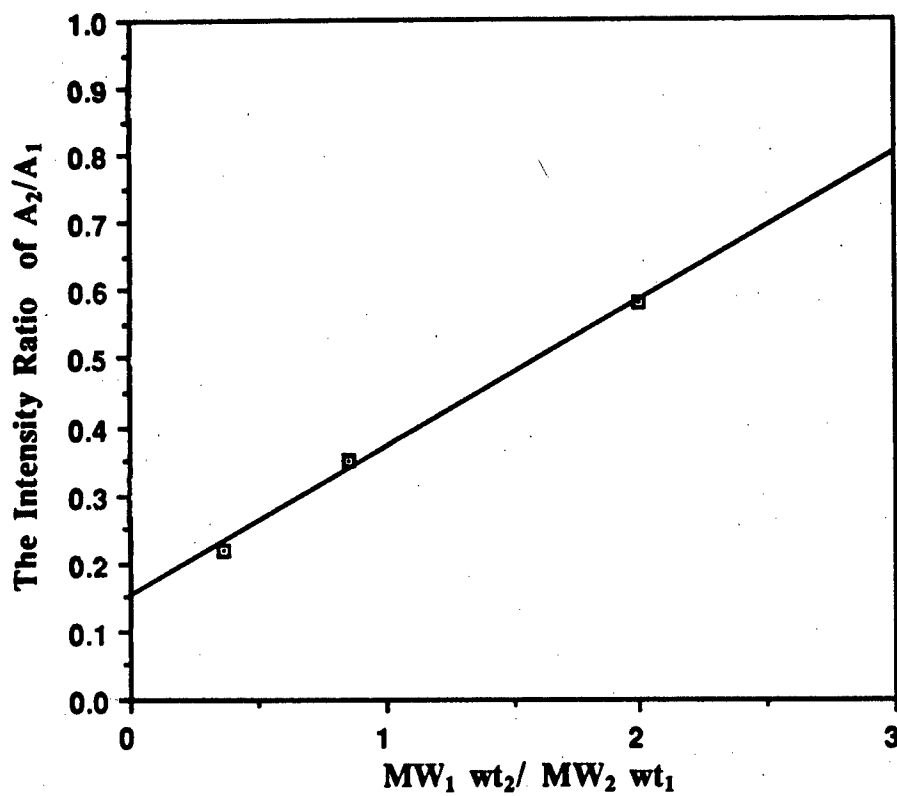Figure 10. PBZT/Lubrizol Composition Calibration Curve Using FTIR

32

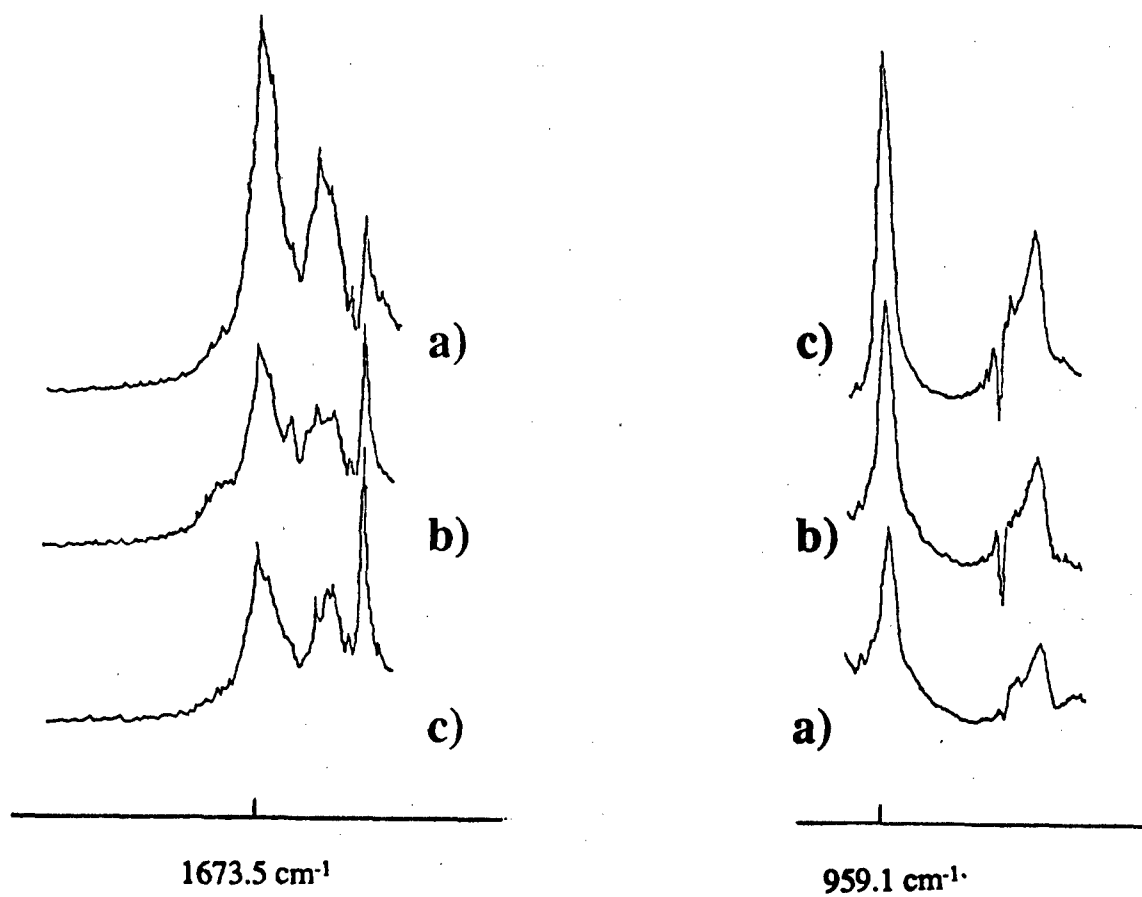Figure 11. The Intensity Ratio of A_2/A_1 As a Function of $MW_1 \, wt_2/ MW_2 \, wt_1$

Figure 12. FTIR Spectra of Different PBZT/Lubrizol Coagulated Blends at 1673.5 cm^{-1} and 959.1 cm^{-1}; a) 30/70 , b) 50/50 , and c) 70/30 PBZT/Lubrizol blends

stretching band around 1673.5 cm^{-1} becomes smaller and the PBZT characteristic absorption around 959.1 cm^{-1} becomes stronger.

By measuring area of above two characteristic spectrums of coagulated PBZT/Lubrizol blends, the composition variations after coagulation were calculated and are shown in Table 3, and all the composition ratio of PBZT/Lubrizol is expressed as wt. %. The PBZT/Lubrizol coagulated compositions from solutions just below the critical concentration, such as 5.5 % 50/50, 4.0 % 70/30, and 9.98 % 30/70 PBZT/Lubrizol blends, are the same as the initial composition. This could be due to the molecular entanglement between PBZT and Lubrizol or the ionic intermolecular interaction between two components. The isotropic solution morphology just below the critical concentration is directly transformed to the solid state during through the molecular interaction. However, when the concentration is far below or above the critical concentration, the coagulated compositions show different composition from the initial composition. This is due to either the heterogeneity of solution morphology which has the PBZT molecular domains in the Lubrizol components or the free Lubrizol which is soluble in the water.

For 9.98 % 30/70 and 5.44 % PBZT/Lubrizol blends, both coagulated films yielded a lower Lubrizol content. It is possible that below a certain rod-coil ratio, there are insufficient rod content to interact or entangle with all the Lubrizol present. The excess Lubrizol which does not interact with PBZT should be dissolved out in water during coagulation. Another interesting result to notice is that both 7.61 % 50/50 and 5.6 % PBZT/Lubrizol coagulated blends show the same PBZT/Lubrizol composition of 40/60 wt. % which corresponds to 33/67 molar ratio of PBZT and Lubrizol components. When the PBZT and Lubrizol are dissolved in MSA solvent, the ionic interaction is formed between the protonated PBZT molecules and the anionic sulfonic groups from both MSA and Lubrizol. If the interaction is exclusively between the PBZT and the Lubrizol, the stochiometric molar ratio of ionic species of PBZT and Lubrizol should be 33/67

TABLE 3

SAMPLE COMPOSITION IDENTIFICATION	b_2C_2/b_1C_1	PBZT/LUBRIZOL	
		Before Coagulation	After Coagulation
5.50 wt.%($\leq C_{cr}$) PBZT/Lubrizol	0.37	50/50	51/49
7.61 wt.% (>C_{cr})PBZT/Lubrizol	0.28	50/50	40/60
4.00 wt.% ($\leq C_{cr}$)PBZT/Lubrizol	0.58	70/30	70/30
5.44 wt.% (>C_{cr})PBZT/Lubrizol	0.76	70/30	80/20
5.60 wt.% (<C_{cr})PBZT/Lubrizol	0.27	30/70	39/61
9.98 wt.%($\leq C_{cr}$) PBZT/Lubrizol	0.23	30/70	32/68
Reference Mixture 30/70 PBZT/Lubrizol	0.22	***	***
Reference Mixture 50/50 PBZT/Lubrizol	0.35	***	***
Reference Mixture 70/30 PBZT/Lubrizol	0.58	***	***

b_1 : Absorptivity of Lubrizol Component

C_1 : Concentration of Lubrizol Component

b_2 : Absorptivity of PBZT Component

C_2 : Concentration of PBZT Component

PBZT/Lubrizol mol %. During the coagulation, the ionic network structure is preserved in the solid state and excess amount of Lubrizol without molecular interactions should be dissolved out. The coagulation composition data need further verification, but it is clear that the rod molecule is affecting the solubility of Lubrizol and the critical concentration plays an important role during the coagulation process.

The effect of coagulation time was studied by immersing the coagulated films in the distilled water for 168 hours. The coagulated composition of PBZT and Lubrizol component was calculated from FTIR analysis and was compared with the results of 24 hours coagulation in Table 4. There is no difference of PBZT/Lubrizol composition ratio between 24 hours and 168 hours coagulation. This suggests that within the first 24 hours, most coagulation occurs and the excess Lubrizol component without any intermolecular interaction is dissolved out. Longer coagulation time does not have significant effect on composition ratio of PBZT and Lubrizol in the coagulated blends.

4.3.2. WAXD

WAXD analysis were made for the coagulated blends of PBZT and Lubrizol and analysis result is shown in Table 5. Since these samples were prepared through the hand sheared quenching process, the small orientation effect of PBZT chain crystalline structure along the shear direction could be observed by the 4.0 A d-spacing of moderate arc formation. Most diffraction patterns of the coagulated blends exhibit the certain extent of micro-phase separation during the coagulation process as evidenced by strong reflection pattern corresponding to 3.5 A and 6.1 A d-spacing. Depending upon the concentration of polymers and composition ratio of two components, the coagulated microstructure should be different. Usually, the PBZT/Lubrizol blends coagulated from solutions just below the critical concentration shows less phase separated and less disordered X-ray scattering

37

TABLE 4. Composition Variation of PBZT/Lubrizol Blends With Time

Sample Identification	Initial PBZT/LUBRIZOL Composition	Coagulated in Distilled Water	
		24 Hrs.	168 Hrs.
5.50 wt.% PBZT/Lubrizol	50/50	51/49	50/50
7.61 wt.% PBZT/Lubrizol	50/50	40/60	42/58
4.00 wt.% PBZT/Lubrizol	70/30	70/30	68/32
5.44 wt.% PBZT/Lubrizol	70/30	80/20	76/24
5.60 wt.% PBZT/Lubrizol	30/70	39/61	38/62
9.98 wt.% PBZT/Lubrizol	30/70	32/68	30/70

TABLE 5. WAXD Result of Coagulated Films

Coagulated Film	d-Spacing (A)				
7.61 % 50/50 PBZT/Lubrizol	2.43	3.45	4.06	6.09	11.93
5.50 % 50/50 PBZT/Lubrizol	2.47	3.46	4.08	6.10	11.80
4.00 % 70/30 PBZT/Lubrizol	2.55	3.47	4.09	5.62	11.93
5.44 % 70/30 PBZT/Lubrizol	2.45	3.47	4.12	5.00	12.03
5.60 % 30/70 PBZT/Lubrizol	2.81	3.46	4.07	6.01	11.21
9.98 % 30/70 PBZT/Lubrizol	**	3.43	3.94	5.27	12.17

pattern, compared with those prepared above the critical concentration. However, it is not clear whether the actual molecular level composite was obtained or not.

4.3.3. RHEOLOGY

The viscosity of Lubrizol/MSA solution with varying polymer concentrations was examined in order to study the chain entanglement behavior of Lubrizol in MSA solvent. By measuring the steady shear viscosity with frequency range from 10^{-2} to 10^2 sec^{-1} and extrapolating to zero shear rate, the measured zero shear rate viscosity of Lubrizol/MSA system was obtained and shown as a function of concentration from 1 to 14 wt.% in Figure 12. As seen in Figure 13, the slope of viscosity data exhibits sudden change around 6 wt.% Lubrizol concentration. This indicates that the onset of chain entanglement of Lubrizol component in MSA occurs around 6 wt. % solution. Besides, it was observed during solution preparation that is very difficult to mix and prepare the homogeneous Lubrizol solution above 6 wt.%. Above this concentration, the prepared Lubrizol solution does not show any flow behavior which is almost like a gum structure. This is due to the entangled chain network structure formation of ultra high molecular weight Lubrizol component which prevents the solution flow behavior.

4.4. CONCLUSION

The two polymer system, however clearly showed molecular composite behavior because Lubrizol, which is water soluble, is coagulated along with PBZT from MSA solutions. It is not clear at this point whether the ionic interactions between the two polymers are responsible for the co-coagulation, or they co-coagulate because of chain entanglement between the rod and the very high M.W. Lubrizol. Additional data are needed to address these issues.
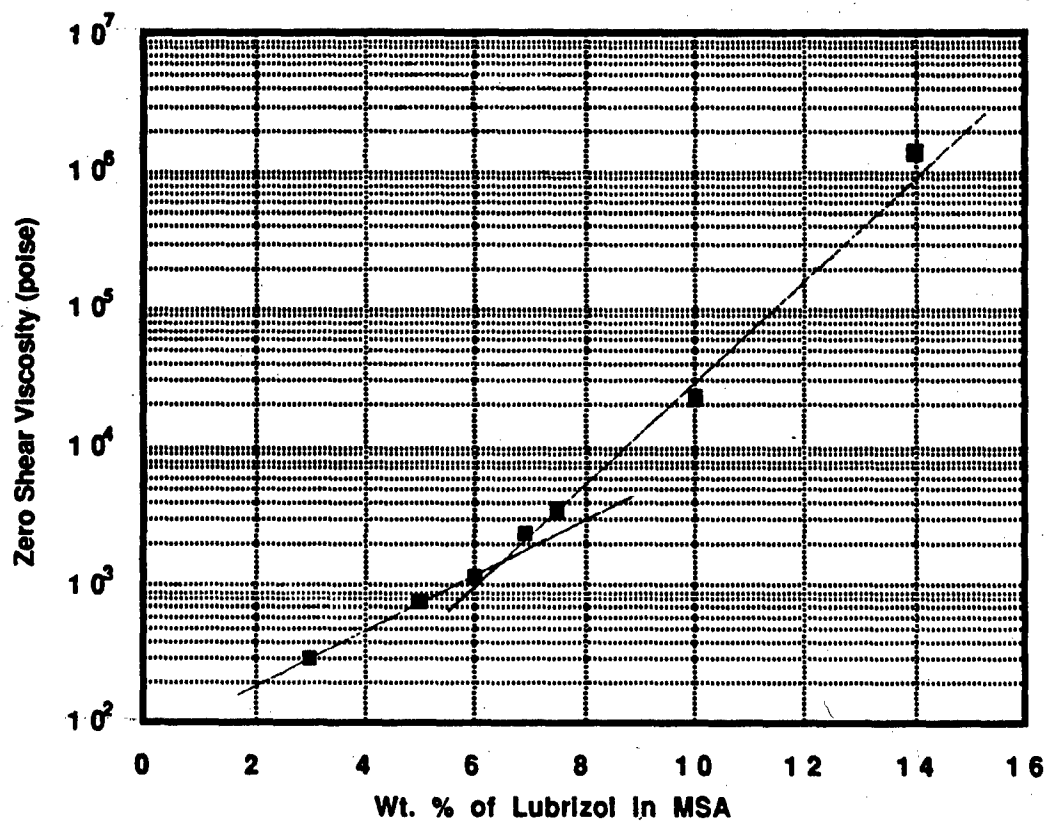
Figure 13. Zero Shear Viscosity of Lubrizol in MSA as a function of Lubrizol wt.%

REFERENCES

1. L.S. Tan, F.E. Arnold, and H. Chuah, to be published

2. T. Helminiak, G. Husman, W. Adams, D. Wiff, and C. Benner, ACS Polymer Preprint, 16(2), 659 (1975)

3. W.F. Hwang, D.R. Wiff, C.L. Benner, and T.E. Helminiak, J. Macro. Sci. Phys., B(22), 231 (1983)

4. K.N. Ptak, K. Gupte, C.Y. Lee, and H. Chuah, ACS PMSE Preprint, 56, 517 (1987)

5. H. Chuah, C.Y. Lee, and T.E. Helminiak, Technical Report AFWAL-TR-87-4127 (1988)

6. A. Crasto, K.M. Gupte, and C.Y. Lee, ACS Polym. Mat. Sci. & Eng., 59, 1101 (1988)

7. C.A. Gabriel, Ph.D. Thesis of University of Massachusetts (1987)

8. D.R. Wiff, W.F. Hwang, H.H. Chuah, and E.J. Soloski, Polym. Eng. & Sci., 27(20), 1557 (1987)

9. P.J. Flory, Macromolecules, 11(6), 1138 (1978)

10. T. Helminiak, M. Wellman, W.F Hwang, V. Rodgers, and C. Benner, Technical Report AFWAL-TR-80-4163 (1981)

11. G.C. Berry, Y. Einaga, R. Furukawa, and H.H. Tsai, Technical Report AFWAL-TR-82-4090 (1982)

12. W. J. Welsh, D. Bhaumik, and J. E. Mark, Macromolecules, 14, 947 (1981).

13. L. S. Tang and F. E. Arnold (to be published).

14. P. J. Flory, Proc. R. Soc. London, Ser. A, 234, 73 (1956).

15. L. Onsager, Ann. N. Y. acad. Sci., 51, 627 (1949).

16. G. C. Berry, P. C. Metzger, S. Venkatraman, and D. B. Cotts, Am. Chem. Soc.

Div. Polym. Chem., 20, 42 (1979)

17. S. Jeneke and S.J. Tibbetts, J. Polym. Sci., Part B, Polym. Phys., 26, 201 (1988)

18. D.N. Rao, J. Swiatkiewicz, P. Chapra, S.K. Choshal, and P.N. Prasad, Appl. Phys. Lett., 48, 1187 (1986)

19. Robert M. Silverstein *et al.*, "Spectrometric Identification of Organic Compound", John Wiley & Sons, 1976
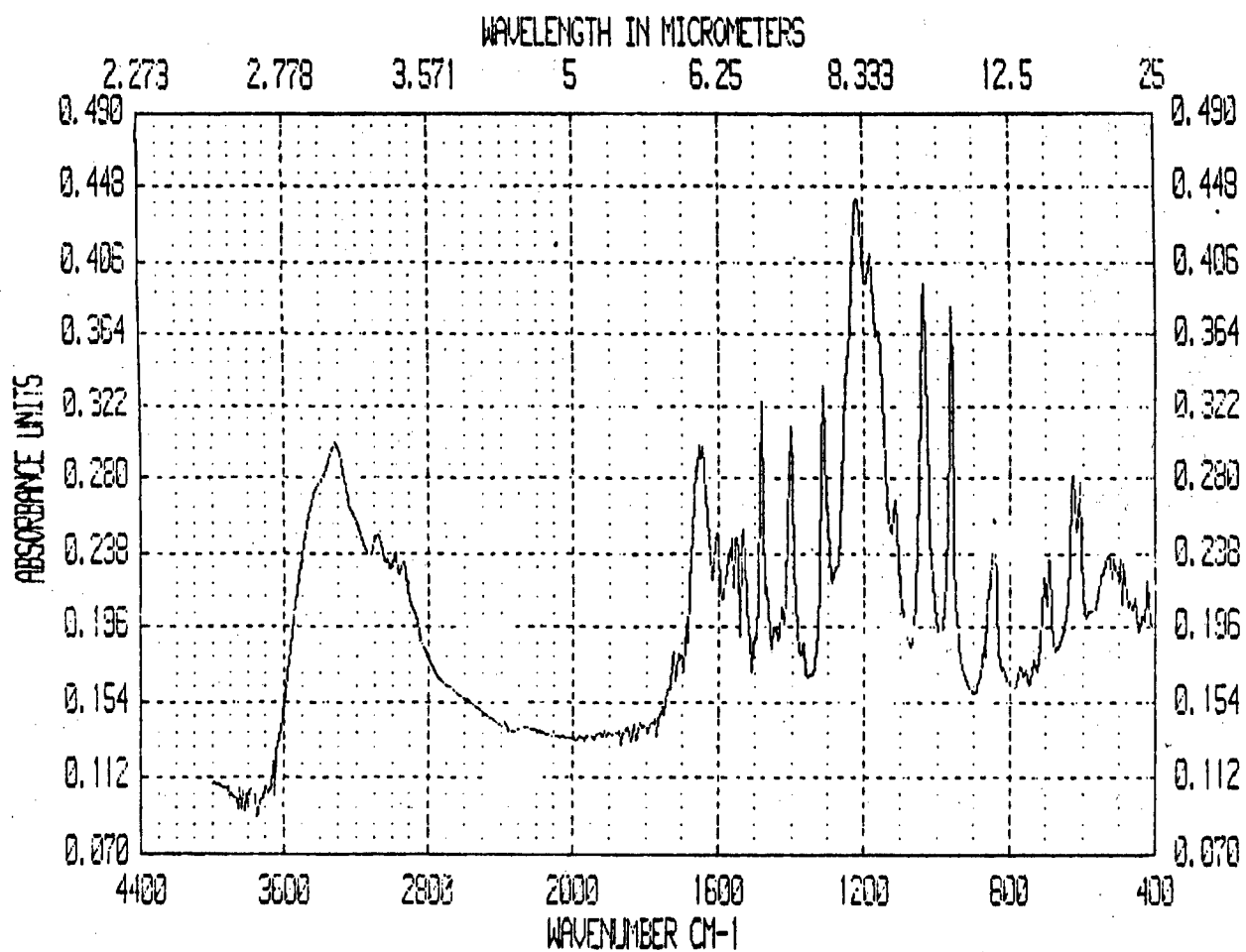
APPENDIX I

IR SPECTRA OF REFERENCE BLENDS

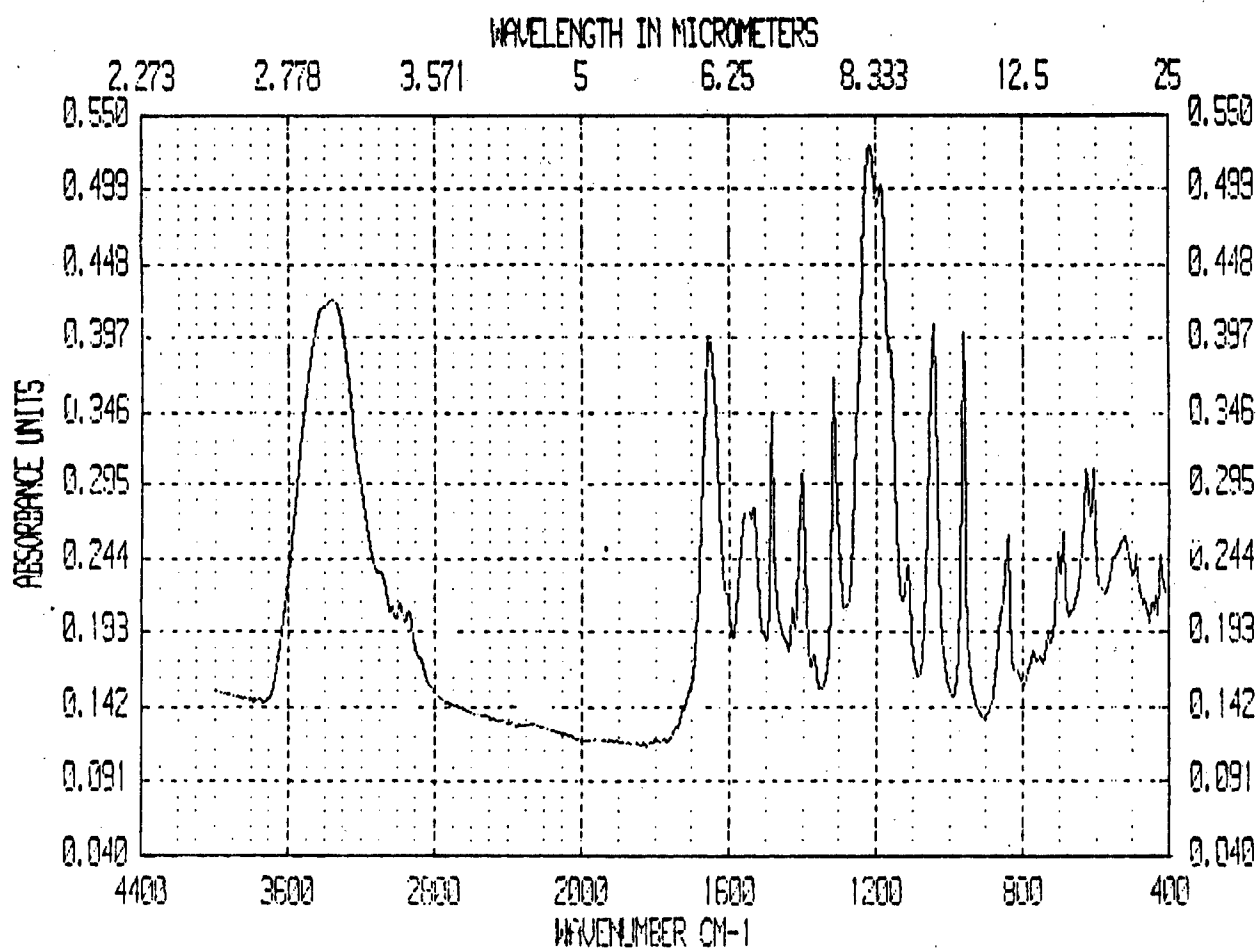Figure 14. FTIR Spectrum of 30/70 PBZT/Lubrizol Reference Blend

Figure 15. FTIR Spectrum of 50/50 PBZT/Lubrizol Reference Blend

46
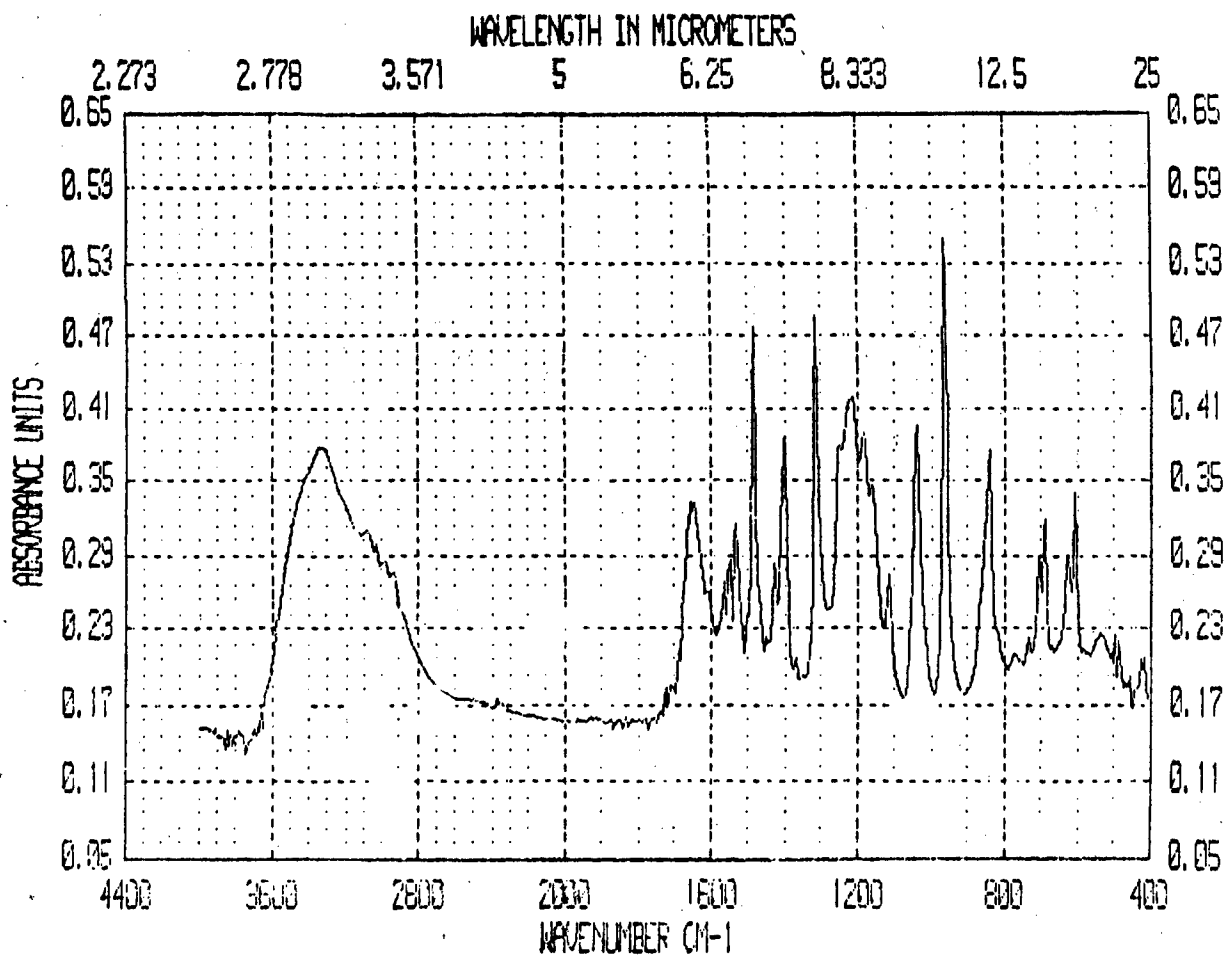
Figure 16. FTIR Spectrum of 70/30 PBZT/Lubrizol Reference Blend

APPENDIX II

IR SPECTRA OF COAGULATED BLENDS
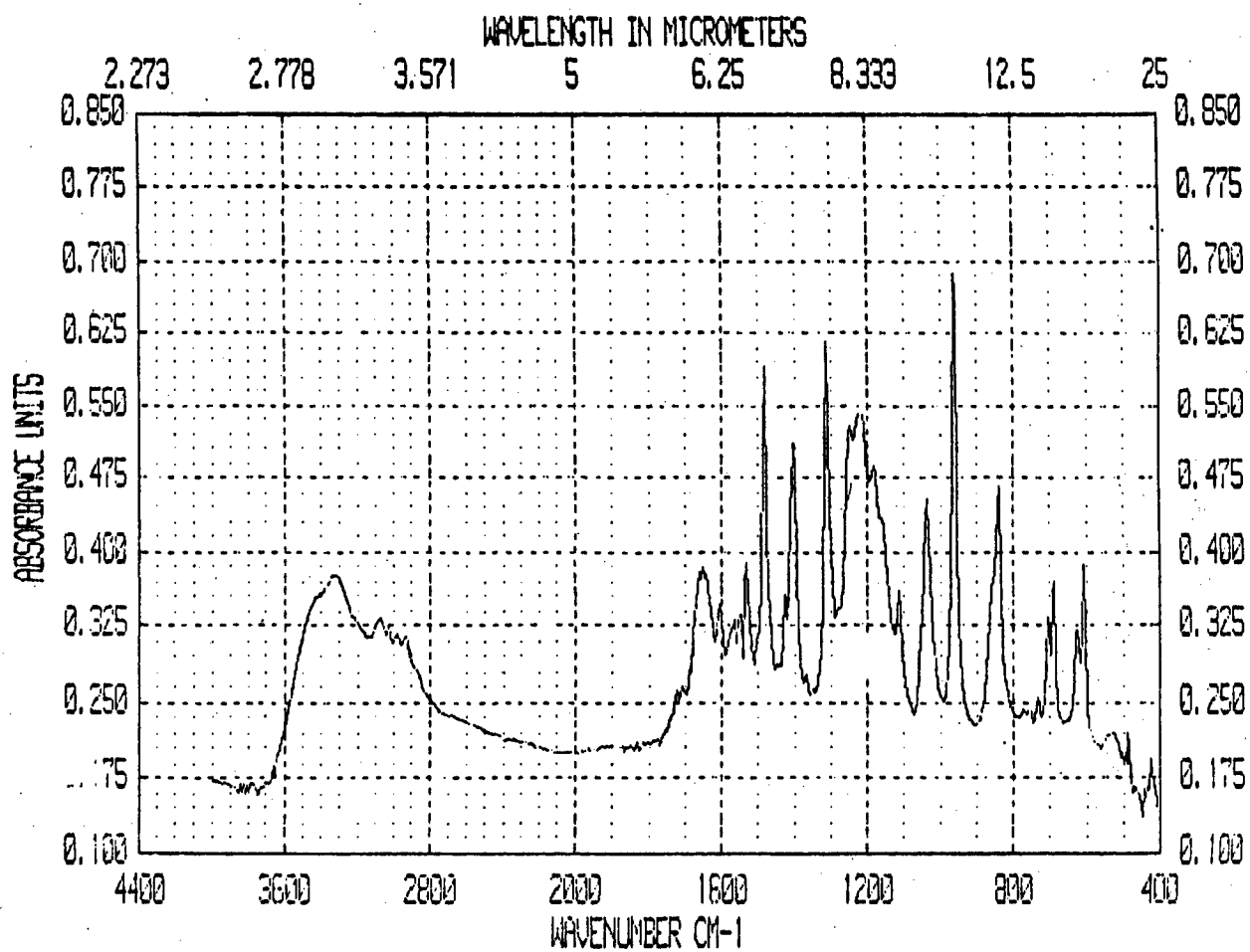
Figure 17. FTIR Spectrum of 5.5 WT.% 50/50 PBZT/Lubrizol Coagulated Blend
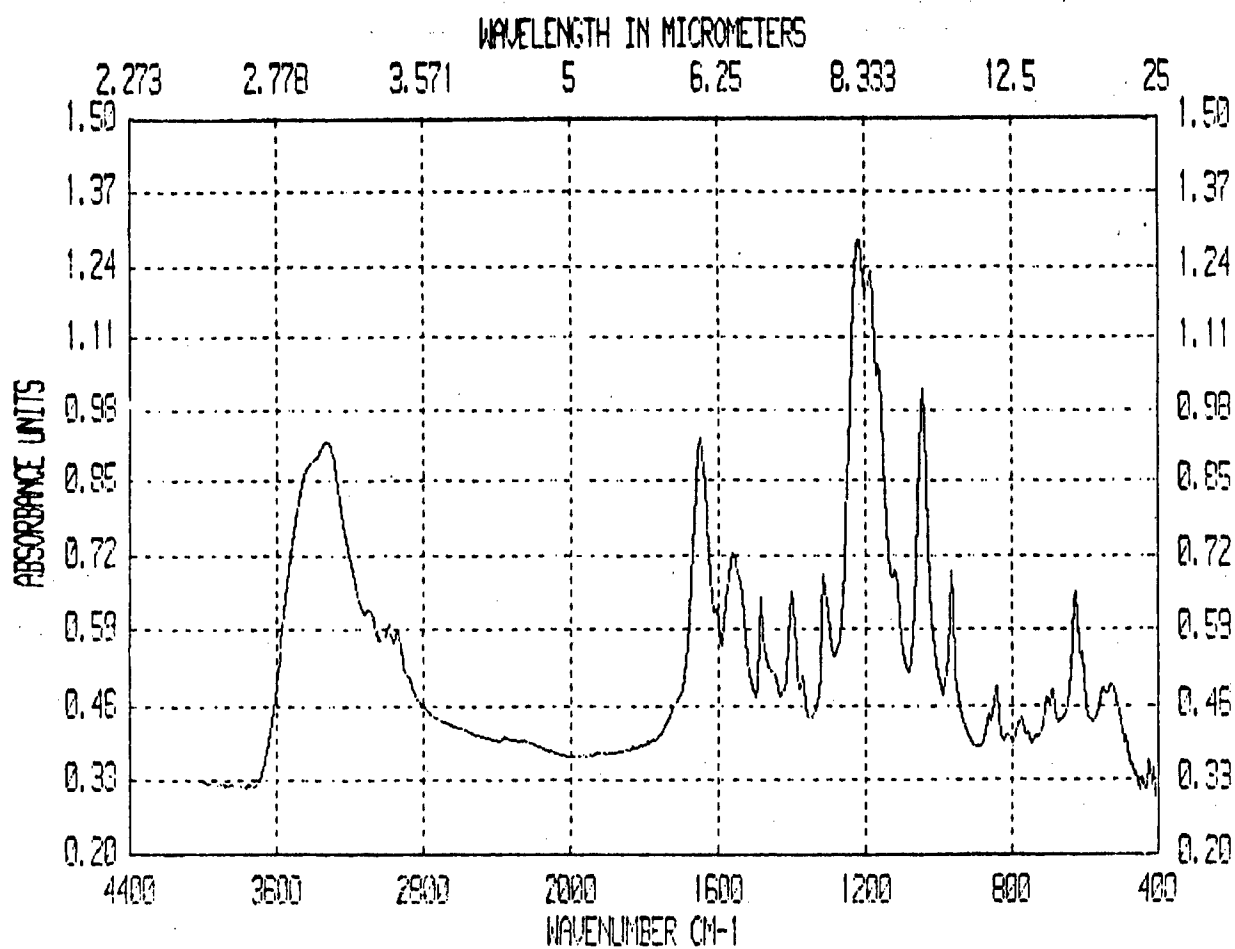
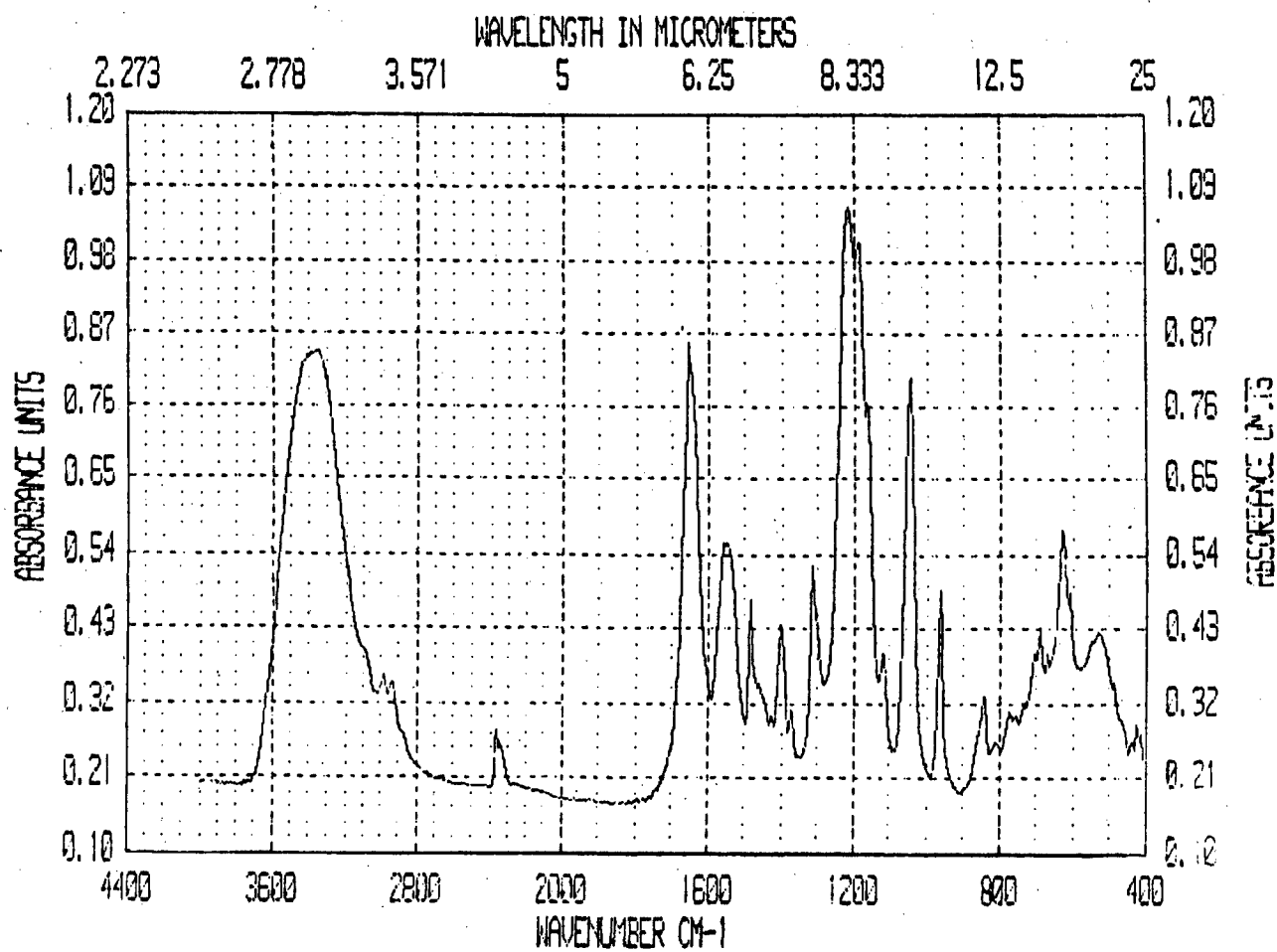Figure 18 FTIR Spectrum of 7.6 WT.% 50/50 PBZT/Lubrizol Coagulated Blend

Figure 19. FTIR Spectrum of 4.0 WT.% 70/30 PBZT/Lubrizol Coagulated Blend
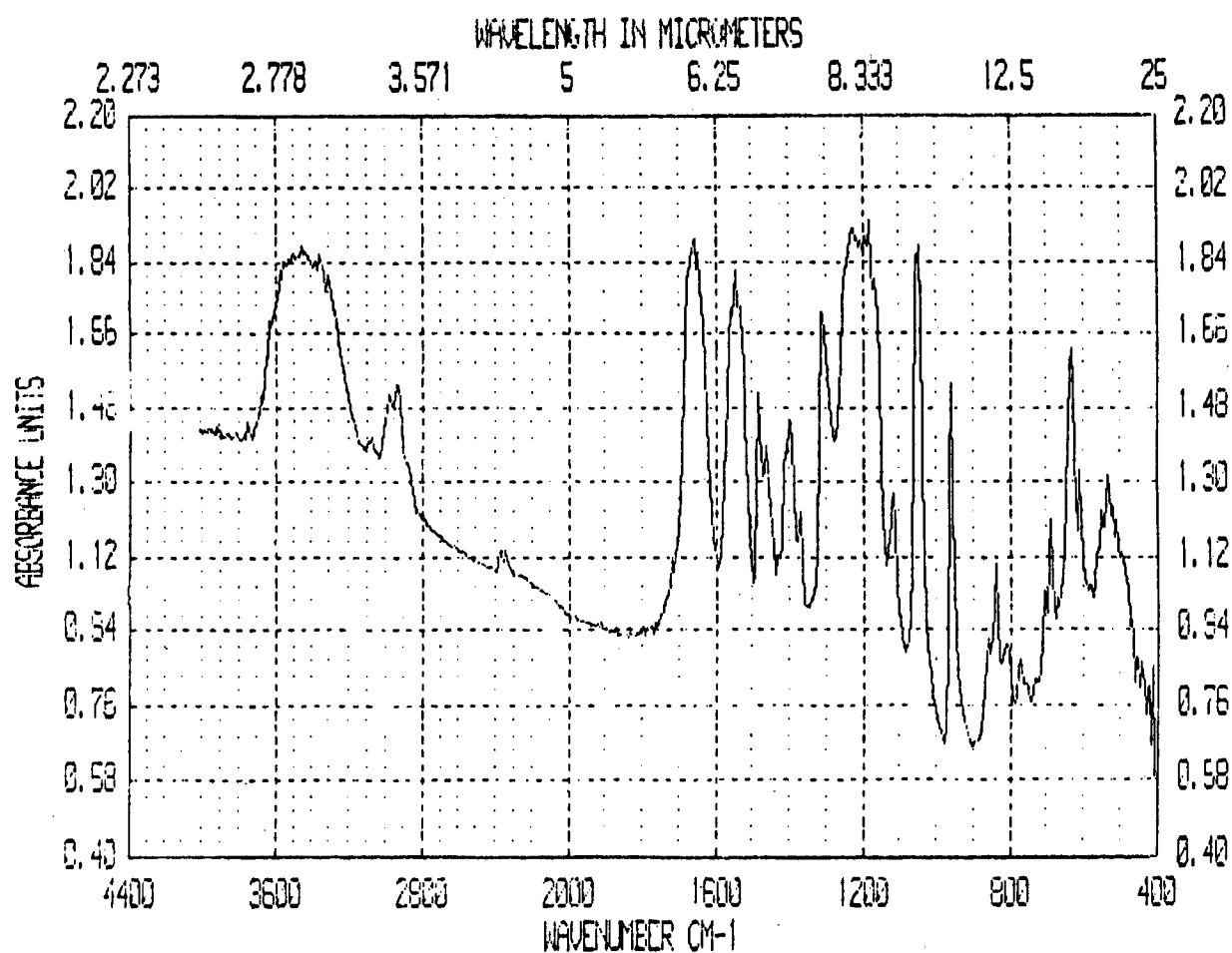
51

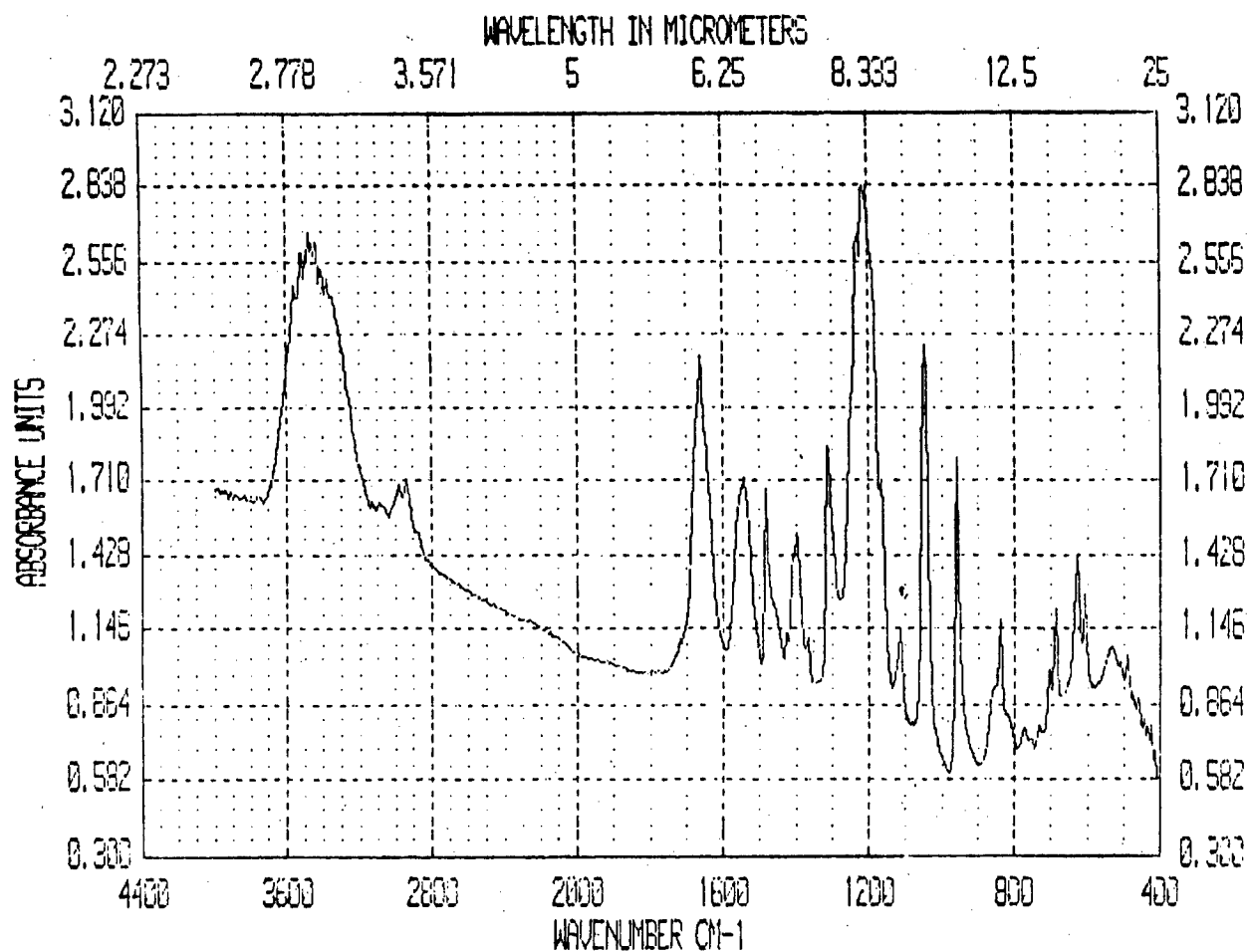Figure 20. FTIR Spectrum of 5.4 WT.% 70/30 PBZT/Lubrizol Coagulated Blend

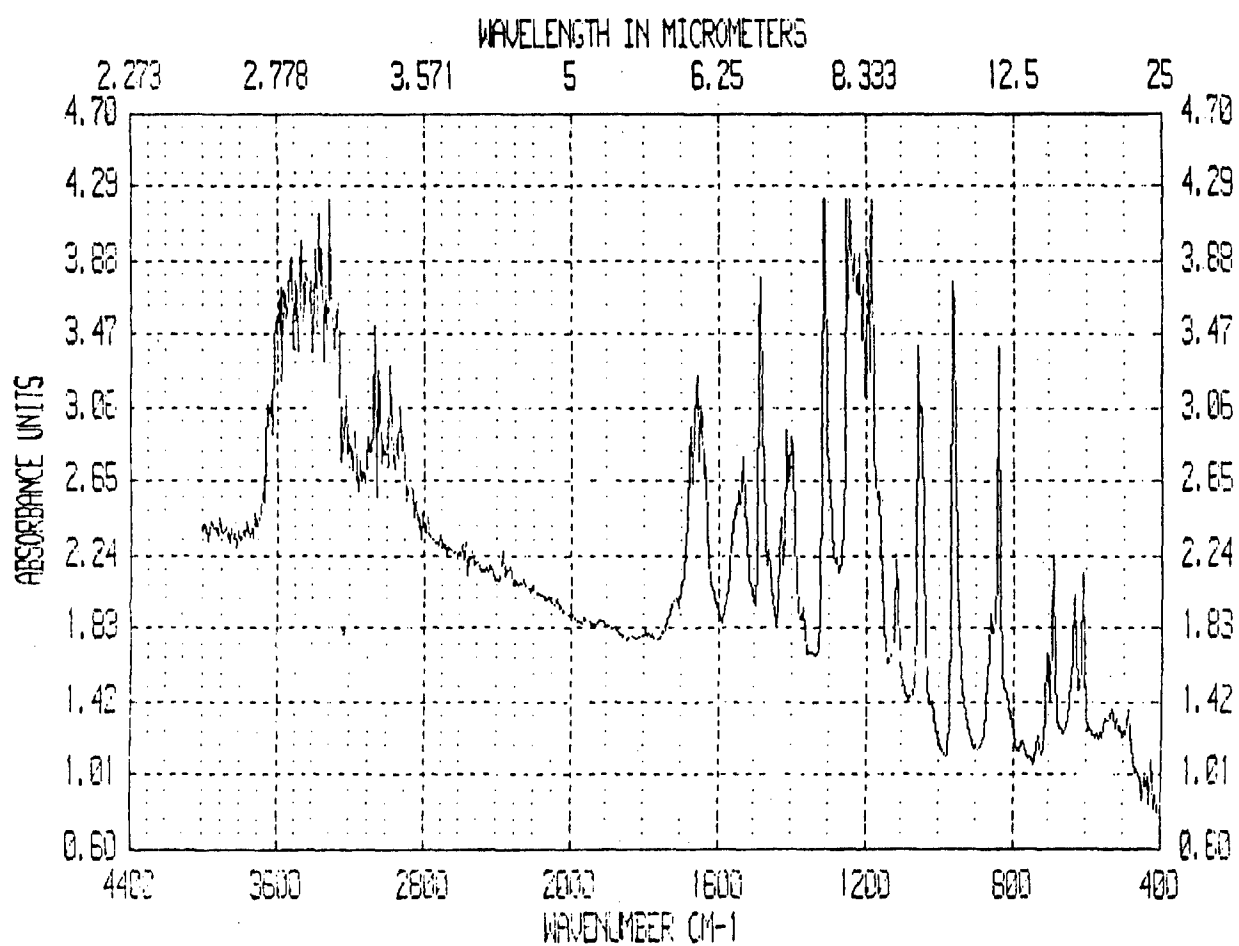Figure 21. FTIR Spectrum of 5.6 WT.% 30/70 PBZT/Lubrizol Coagulated Blend

Figure 22. FTIR Spectrum of 9.9 WT.% 30/70 PBZT/Lubrizol Coagulated blends